Sustainable Approach for Cellulose Aerogel Preparation from the DBU–CO 2 Switchable Solvent

Kelechukwu Onwukamike, Laurine Lapuyade, Laurence Maillé, Stéphane Grelier, Etienne Grau, Henri Cramail, Michael A.R. Meier

Sustainable Approach for Cellulose Aerogel Preparation from the DBU–CO_2 Switchable Solvent

Kelechukwu N. Onwukamike, Laurine Lapuyade, Laurence Maillé, Stéphane Grelier, Etienne Grau, Henri Cramail*, Michael A.R. Meier*

Abstract

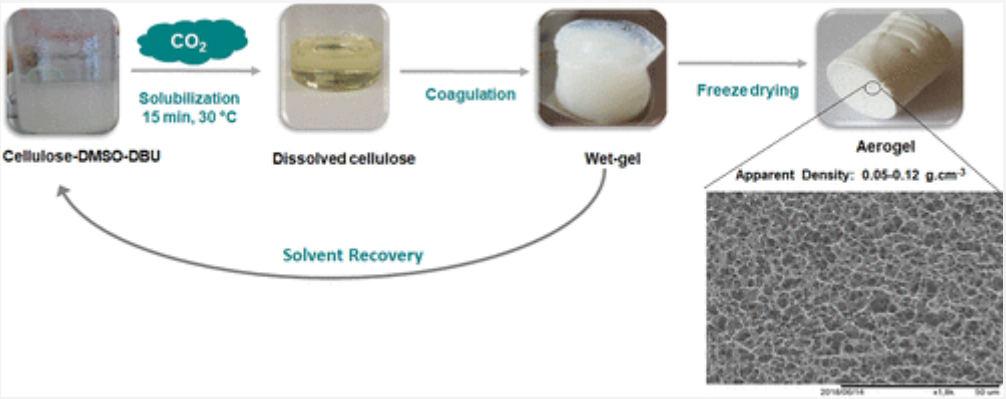

We report a sustainable and easy approach for the preparation of cellulose-based aerogels from the DBU–CO_2 switchable solvent system via a solubilization and coagulation approach followed by freeze-drying. The easy, fast, and mild solubilization step (15 min at 30 °C) allows for a rapid preparation procedure. The effect of various processing parameters, such as cellulose concentration, coagulating solvent, and the superbase, on important aerogel characteristics including density, porosity, pore size, and morphology, were investigated. Density values obtained ranged between 0.05 and 0.12 g/cm^3, with porosity values between 92% and 97%. The morphology of the obtained cellulose aerogels was studied using scanning electron microscopy (SEM) showing a random and open large macroporous cellulose network with pore sizes ranging between 1.1 and 4.5 µm, depending on the processing conditions. In addition, specific surface areas determined by N_2 adsorption applying the BET equation ranged between 19 and 26 m^2/g. The effect of the coagulating solvent and superbase on the crystallinity was investigated using X-ray diffraction (XRD) showing an amorphous crystal structure with a broad 2θ diffraction peak at 20.6°. In addition, no chemical modification was observed in the prepared aerogels from infrared spectroscopy. Finally, the recovery and reuse of the solvent system was demonstrated, thus making the process more sustainable.

Synopsis

An easy and sustainable approach for the preparation of cellulose aerogels from the DBU−CO_2 switchable solvent system demonstrates solvent recovery during aerogel preparation.

Introduction

As the most abundant organic polymer in nature, cellulose is a potential and viable replacement for the unsustainable fossil-based polymers being used today. However, as cellulose has no thermal transition or melting point, direct processing is not possible.(1) However, cellulose can be shaped into various forms through solubilization and subsequent regeneration. Viscose, the most common and industrially relevant material used for the preparation of regenerated cellulose fibers with diameters of 10 microns, is made in this way.(1) In this case, cellulose is solubilized by first transforming it to a xanthate in alkaline medium using CS_2, resulting in viscose, which is then regenerated in acidic solution.(1) Other cellulose objects, such as highly porous beads,

have been reported being made from 8% NaOH–water mixtures(2) or from NaOH–urea–water mixtures.(3) Recently, Budtova and co-workers reported on the preparation of cellulose beads by employing JetCutting technology from the $[DBNH]^+[AcO]^-$ ionic liquid.(4) Of interest for the present report are the so-called cellulose-based aerogels (aero-cellulose).

Aerogels are classified as materials with highly porous structures and voids filled with gases such as air; they show very low densities and a high specific surface area.(5,6) They are usually obtained from their wet gels by drying in a way that maintains their pores. Examples of such drying procedures include freeze-drying or drying with supercritical CO_2. In this way, the strong capillary forces, which will otherwise lead to a collapse of the structure during drying, are overcome. The most common inorganic aerogels are based on silica,(5) whereas resorcinol–formaldehyde-based aerogels are the most common organic representatives made via the sol–gel process.(7,8) Aerogels are a very interesting class of material, finding applications as thermal insulators,(9) as electrodes for electrochemical applications (after pyrolysis),(10) and for biomedical use (controlled drug release or as scaffolds).(11,12) Interestingly, aerogels can also be prepared from cellulose with the first attempt reported by Kistler in the 1930s.(13,14) Reports on aerogel preparation from cellulose I, such as bacterial cellulose or micro- or nanofibrillated cellulose, are available.(10,15,16) Silylated cellulose nanofibril sponges have been reported to be able to selectively remove oil from water.(17) On the other hand, the use of regenerated cellulose (cellulose II, for instance from agricultural waste sources) offers a cheaper and more viable source of cellulose for aerogel preparation. For the production of bacterial cellulose fibers, for instance, high amounts of nutrients are required. Most importantly, regenerated cellulose can be prepared from various cellulose types without the need for further preparation procedures (in contrast to nanocellulose). For cellulose II, the aerogels are made via the solubilization and coagulation approach. The procedure is explained briefly as follows: cellulose is solubilized first, followed by transferring into a mold where a nonsolvent (examples are water, methanol, ethanol, isopropanol, or others) is added to exchange the higher-boiling cellulose solvent. After solvent exchange, depending on the drying method being employed, a second solvent exchange might be necessary. For example, for supercritical CO_2-drying, compatible solvents such as ethanol are used, whereas for freeze-drying water is used instead.

The first and most challenging step of preparing cellulose aerogels from regenerated cellulose II involves a complete solubilization of the polymer. This step is challenging because cellulose is insoluble in common organic solvents as well as in water.(1) This insolubility challenge of cellulose has been attributed to its inherent intra- and intermolecular hydrogen bonding.(1) Thus, only solvents capable of disrupting these hydrogen bonds can solubilize cellulose (cellulose solvents). In this regard, Innerlohinger and co-workers employed *N*-methyl morpholine-*N*-oxide monohydrate ($NMMO \cdot H_2O$) to solubilize cellulose for cellulose aerogel preparation.(5) Factors such as cellulose concentration and preparation methods were investigated regarding their influence on the density and volume shrinkage of the obtained aerogels. Their results showed that increasing cellulose concentrations generally led to an increase in the density. They reported aerogel density values between 0.02 and 0.2 g/cm^3 with an open-pore nanofibrillar aerogel morphology typical for supercritical CO_2-drying. Following a similar cellulose aerogel preparation approach, Wang et al. used an 8% LiCl–DMSO solvent mixture for cellulose solubilization and subsequent coagulation in ethanol.(18) To aid the solubilization step, the cellulose was first activated by soaking in ethylenediamine (EDA) for 24 h at room temperature, with dissolution achieved after heating to 75 °C for 24 h. The resulting solubilized cellulose solution was then coagulated using ethanol and dried via supercritical CO_2 to afford the desired aerogel. The obtained densities ranged from 0.068 to 0.137 g/cm^3 with mesoporous structures containing pore sizes ranging between 10 and 60 nm. The use of a salt melt based on calcium thiocyanate ($Ca(SCN)_2 \cdot 4H_2O$) has been reported separately by Hoepfner et al.(19) and Jin et al.(20) In their reports, cellulose was solubilized between 110 and 140 °C within 1 h. As with the previous procedures, coagulation was achieved using water or ethanol for freeze-drying or supercritical CO_2-drying, respectively. The obtained aerogels showed an increase in density with increased cellulose concentrations, as well as a nanofibrillar structure for the supercritical CO_2-dried samples.(19,20)

A more detailed study on the structure development and morphology control of cellulose aerogels was reported by Budtova and Buchtová.(21) In their report, cellulose solubilization was achieved in an ionic liquid–DMSO solvent mixture. Here, the ionic liquid EMIMAc (1-*N*-ethyl-3-methyl imidazolium acetate) was used. After cellulose dissolution, the general coagulation approach was applied using ethanol. Various drying methods were investigated such as vacuum, freeze-drying, and supercritical CO_2-drying. The authors classified the obtained gels on the basis of the drying method as follows: xerogels (vacuum-dried), cryogel (freeze-dried), and aerogel (supercritical CO_2-dried). As expected, and confirmed by the results obtained, xerogels were completely nonporous, as the high capillary forces during drying led to a collapse of the porous structure. The xerogels had very high density values close to those of microcrystalline cellulose (∼1.5 g/cm^3).(22) On the other hand, the porous structure of the gels was kept in the case of freeze-dried or supercritical CO_2-dried samples with porosities between 86% and 96%. Of importance to note was the difference in the density as well as the volume shrinkage between both drying methods. Aerogels obtained from freeze-drying showed less volume shrinkage (before and after drying) compared to supercritical CO_2-drying. In addition, lower density values (typically below 0.1 g/cm^3) were obtained for freeze-dried gels compared to values between 0.1 and 0.2 g/cm^3 for supercritical CO_2-dried samples.(21)

The effect of various cellulose solvents on the morphology and properties of cellulose aerogels has been reported by Liebner and co-workers.(23) Solvents investigated included ionic liquid/DMSO (EMIMAc–DMSO), tetrabutyl-ammonium fluoride/dimethyl sulfoxide (TBAF–DMSO), *N*-methyl morpholine-*N*-oxide monohydrate (NMMO·H_2O), and calcium thiocyanate octahydrate–lithium chloride and CTO ($Ca(SCN)_2·8H_2O$–LiCl). The solubilized cellulose was coagulated using ethanol followed by supercritical CO_2-drying to afford the desired aerogels. Their result showed that these solvents played a significant role in the bulk properties of the aerogels such as morphology and porosity. For instance, while aerogels made from EMIMAc–DMSO showed a more random short nanofiber network that assembled into a globular superstructure, those from TBAF–LiCl showed a more homogeneous interwoven nanofiber network with interconnected nanopores. On the other hand, aerogels from NMMO·H_2O and CTO showed a more random network of cellulose nanofibers. The authors correlated these differences to the mechanism of cellulose network formation in these different solvents. On one hand, aerogels from EMIMAc and TBAF–LiCl followed the spontaneous one-step phase separation mechanism, which is entirely controlled by diffusion. NMMO and CTO-derived aerogels followed a two-step phase separation mechanism. The first phase separation occurs during the cooling of the solubilized cellulose solution, which gives time for an alignment of the cellulose fibers into longer nanofibers. The second phase separation step occurs during the addition of the nonsolvent (coagulating solvent), which also leads to further alignment of the cellulose fibers in close proximity to the already ordered longer nanofiber networks from the first phase separation step. The effect is an increased crystallinity (cellulose II) and better mechanical properties (higher compressional stress) of the resulting aerogels.(23) It is also important to mention that, apart from phase separation, gelation is another mechanism to form cellulose networks. A typical example is the use of solvents such as 8% NaOH–water mixtures.(2) In such solvents, depending on the cellulose concentration and temperature, the cellulose solutions start gelling with time because of the increasing proximity of the hydroxyl groups present in the polymer, thereby leading to hydrogen bonding.

As seen in these previous studies, the used solvents such as LiCl–DMSO, NMMO, and ionic liquids are either toxic (acute toxicity $LD_{50,rat}$ LiCl = 526 mg/kg), thermally unstable,(24,25) or noninert,(26,27) respectively. Furthermore, no investigation on the recycling or reuse of any of these solvents has been reported. In the course of our research on cellulose, sustainability has been one of the most important aspects. As renewability is not enough to ensure sustainability,(28) neglecting other aspects of Green Chemistry(29,30) during cellulose transformation simply shifts the carbon footprint to other stages of the life cycle. In this regard, the easily recyclable and cheaper CO_2 switchable solvent system first reported by Jessop et al.,(31) and adapted for cellulose solubilization independently by the groups of Jerome(32) and Xie,(33) is interesting. Cellulose dissolution in this solvent system can be achieved via two approaches: derivative and nonderivative. In the derivative approach, the cellulose is first activated by a superbase (such as DBU; 1,8-diazabicyclo[5.4.0]undec-7-

ene), allowing their reaction with CO_2 leading to the formation of a DMSO-soluble cellulose carbonate species *in situ*.(32) In the nonderivative approach, simple alcohols such as methanol, hexanol, or ethylene glycol in the presence of a superbase react with CO_2 to form a DMSO–carbonate species solvent system that can solubilize cellulose.(33) These two approaches are shown in Scheme 1. The reversibility/switchability aspect of this solvent system arises from the change in their polarity from nonpolar to polar by addition of CO_2. Upon release of CO_2, the formed polar solvent reverses to their initial nonpolar state.(31) In a more general sense, this class of solvents is similar to the distillable ionic liquids (*N*,*N*-dimethylammonium-*N*′,*N*′-dimethylcarbamate, DIMCARB) described by MacFarlane et al., from the reaction between dimethylamine and CO_2.(34) The as-described solvent was used to extract tannins from certain plants, but could not dissolve cellulose. Kilpeläinen et al. reported an adaptation of this solvent system by using a 1:1 molar ratio between an organic superbase (TMG) alongside carboxylic acid (acetic acid), to form an acid–base conjugate, $[TMGH]^+[AcO^-]$, capable of dissolving cellulose.(35) Sixta and colleagues have recently developed a similar system by using a 1:1 molar ratio between the organic superbase (DBN) and acetic acid, forming $[DBN]^+[AcO]^-$, now used for spinning cellulose fibers in a process termed Ioncell F,(36) and also recently employed by Budtova et al. to prepare cellulose beads.(4)

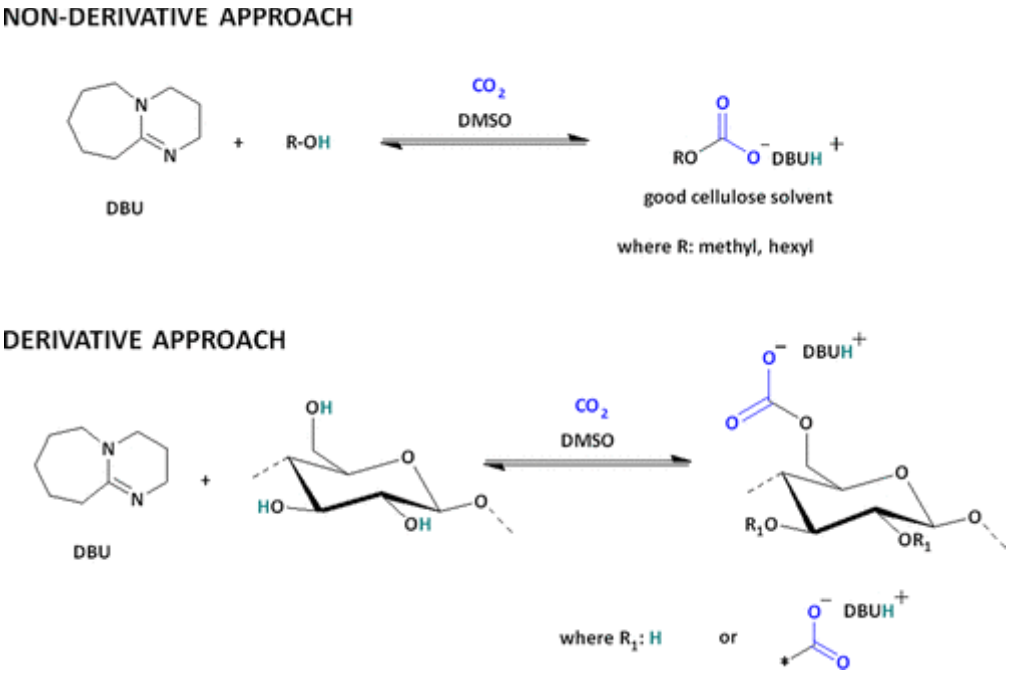

Scheme 1. Nonderivative (top) and Derivative (bottom) Approach of the CO_2 Switchable Solvent System Adapted from Jerome et al.(32) and Xie et al.(33)

By investigating this solvent system in detail, we have been able to further optimize this solvent system, achieving up to 10 wt % cellulose solubilization within 15 min at 30 °C.(37) Having previously reported a more sustainable approach for cellulose derivatization in this solvent via transesterification using plant oils directly(38) as well as very mild succinylation,(39) the question arose if it would be possible to shape cellulose into aerogels from this solvent system following the well-developed solubilization–coagulation approach. Therefore, with this contribution, we report for the first time the preparation of cellulose aerogels from the DBU–CO_2 switchable solvent system. In this case, the cellulose solution was coagulated and subsequently followed by freeze-drying to afford the desired aerogel. The focus herein will be the fast, mild, and easy solubilization step as well as the influence of processing parameters such as the cellulose concentration, coagulating solvent, as well as other superbases on important aerogel characteristics including porosity and morphology. Importantly, as we wish to establish a more sustainable solvent system for cellulose aerogel preparation, the recycling and reuse of the solvent system will be demonstrated. To ease further reading, in the course of this manuscript, we refer to the cellulose solvent as the DBU–DMSO–CO_2 system, whereas the nonsolvents are referred to as water, methanol, ethanol, and isopropanol.

Experimental Section

Materials

Microcrystalline cellulose (MCC, Avicel PH 101) was obtained from Sigma-Aldrich. Cellulose pulp (CP) was purchased from Rayonier Advanced Materials Company (Tartas Biorefinery) and was produced by ammonium sulfite cooking and bleached with an elementary chlorine-free (ECF) process (purity in α-cellulose is 94%). All cellulose samples were dried at 100 °C for 24 h under vacuum to remove free water before use. The 1,8-diazabicyclo[5.4.0]undec-7-ene, DBU (99%); 1,5-diazabicyclo[4.3.0]non-5-ene, DBN (98%); and 1,1,3,3-tetramethylene guanidine, TMG (99%), were purchased from Alfa Aesar. Carbon dioxide was obtained from Air Liquide (>99.9%) and dimethyl sulfoxide (DMSO) from VWR (99%). The following chemicals were used without further purification: ethanol (96%), methanol, and isopropanol.

General Procedure for Cellulose Aerogel Preparation from the CO_2 Switchable Solvent System

Cellulose (0.25 g, 1.5 mmol of anhydroglucose unit, 5 wt %) was stirred in DMSO (5 mL) followed by addition of the superbase (DBU = 0.7 g, TMG = 0.53 g, DBN = 0.57 g; 4.5 mmol, 3 equiv per anhydroglucose unit). The cloudy suspension was transferred to a steel pressure reactor, where 5 bar of CO_2 was applied at 30 °C (40 °C for DBN and TMG) for 15 min. The obtained clear cellulose solution was transferred to a cylindrical-shaped glass mold (diameter 2.2 cm). A 30 mL portion of the corresponding antisolvent (water, methanol, ethanol, or isopropanol) was added slowly from the top and allowed to coagulate over a period of 24 h. Next, the nonsolvent was decanted and changed repeatedly until it contained no sign of DMSO or superbase (from IR spectroscopy). The wet-precursors now filled with the nonsolvent (if different from water) were exchanged to water to allow for freeze-drying. The samples were frozen using liquid N_2 before being placed under a freeze-dryer for 24 h. The aerogel obtained was then stored inside a vacuum desiccator containing P_4O_{10} as a water absorbent prior to further characterization.

Instruments

Freeze-Dryer

The samples were dried using an Alpha 1-2 LD_{plus} model freeze-dryer from CHRIST.

IR Spectroscopy

Infrared spectra of all samples were recorded on a Bruker Alpha-p instrument using ATR technology within the range 4000–400 cm^{-1} with 24 scans.

X-ray Diffraction (XRD) Measurements

X-ray diffraction (XRD) patterns were collected on a PANalitycal X'pert MPD-PRO Bragg–Brentano θ–θ geometry diffractometer equipped with a secondary monochromator and an X'celerator detector over the angular range 2θ = 8–80°. Each acquisition lasted for 1 h and 27 min. The Cu Kα radiation was generated at 45 kV and 40 mA (λ = 0.154 18 nm). The cellulose aerogel samples were prepared on silicon wafer sample holders (PANalytical zero background sample holders) and flattened with a piece of glass.

Scanning Electron Microscopy (SEM)

The surface morphologies of the prepared cellulose aerogels were measured using a HITACHI TM-1000 tabletop microscope. Prior to the measurements, the samples were made conducting by metallization using Au (30 s, 35 mA). From the SEM results, the pore sizes of the aerogels were estimated using ImageJ software by taking the average of 60 randomly selected pore sizes.

Density Measurement

The density (apparent or bulk) of the samples was estimated gravimetrically by taking the ratio of the weight of the samples to their measured volume. An average of 2–4 samples for the same formulation was considered.

Specific Surface Area

The specific surface area of the aerogel samples was determined by measuring N_2 adsorption isotherm at 77 K with an ASAP 2010 instrument from Micrometrics, and applying the Brunauer–Emmett–Teller (BET) equation. The samples were measured after degassing at ambient temperature between 17 and 25 h.

Solvent Recovery

The study of solvent recovery was performed using methanol as the nonsolvent for coagulation after cellulose solubilization in the DBU–DMSO–CO_2 solvent system. After coagulation was complete, the obtained wet sample was repeatedly washed using methanol, and the methanol was recovered quantitatively via rotary evaporation. The remaining fraction in the flask containing DMSO, DBU, and $DBUH^+$ was extracted with cyclohexane. The obtained cyclohexane and DMSO-rich phases were separated. The cyclohexane phase was subjected to the rotary evaporator (45 °C, 200 mbar) leading to a quantitative recovery of cyclohexane, whereas a pure DBU remained in the flask. DMSO was recovered from the DMSO-rich phase through vacuum distillation (90 °C, 25 mbar). This way, a separation from the remaining $DBUH^+$ (alongside HCO_3^- from a possible reaction between water present in DMSO and CO_2) that could not be extracted using cyclohexane was achieved. The recovered DMSO (recovery yield 90%) and DBU (recovery yield 60%) could be used for new cellulose solubilization without any observed difference compared to new reactants.

Results and Discussion

Proposed Mechanism of Cellulose Network Formation

The preparation of aerogels from regenerated cellulose has been proposed to occur via two main mechanisms: phase separation and gelation, depending on the type of solvent employed.(2,23) Phase separation can occur through either a one-step or two-step mechanism. As shown from the reports of Liebner et al.,(23) solvents such as ionic liquids and TBAF–LiCl follow the one-step phase separation mechanism, whereas NMMO·H_2O and CTO ($Ca(SCN)_2 \cdot 8H_2O$–LiCl) follow the two-step phase separation. In the herein-reported CO_2 switchable solvent system, one can assume that the removal of CO_2 will lead to an initial aggregation (caused by interaction between the cellulose fibers and similar to the cooling-induced phase separation described by Liebner et al.(23)), whereas the second phase separation occurs during the noncellulose solvent addition. Phase separation is most likely the mechanism in play for the cellulose network formation in this solvent system and certainly not gelation (direct formation) observed in the solvent such as 8% NaOH–water mixtures, which results from the gelling of the cellulose solution upon increasing the cellulose concentration or temperature. The general cellulose aerogel preparation approach employed for the current study is shown in Scheme 2.

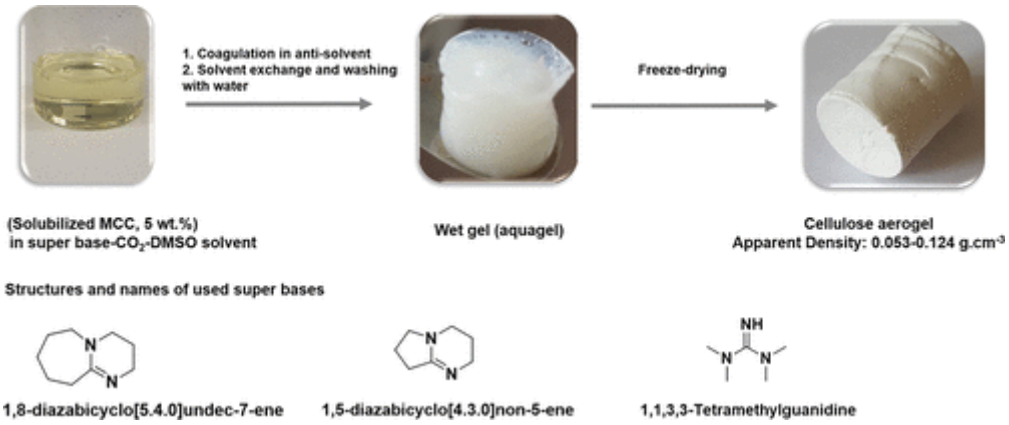

Scheme 2. General Procedure for Cellulose Aerogel Preparation from DMSO–Superbase–CO_2 Switchable Solvent System

Apparent Density (Bulk Density)

Density is one of the most important properties of aerogels, with reported values ranging between 0.002 and 0.3 g/cm^3.(10,21) Such low densities arise from the fact that most of the material's volume is occupied by air. Therefore, the drying process is relevant during the aerogel preparation. In this regard, freeze-drying or supercritical CO_2-drying are recommended, as they avoid pore collapse. In the course of this project, freeze-drying was selected, as it has been reported to result in less volume shrinkage compared to supercritical CO_2-drying.(21) In addition, freeze-dried aerogels have been reported to have lower densities compared to their supercritical CO_2-dried counterparts,(21) as well as provide a faster approach for aerogel preparation. To avoid any misunderstanding, it is also important to point out the limitation of this approach, such as the influence of ice crystals formed during water freezing that might "disturb" the already formed cellulose network of the aerogel. One way to at least limit this influence (by reducing the ice crystal size) is to dip the sample into liquid nitrogen before subjecting it to freeze-drying.(19) The apparent density (also referred to as bulk density in some reports)(5) of the aerogels was determined gravimetrically as in previous reports by taking the ratio between the measured weight to its volume.(5,19) For each formulation, 2–4 measurements were performed, and their average value was considered.

The effect of various processing parameters such as cellulose concentration, coagulating solvent, and the superbase on the apparent density was investigated. In the first instance, the effect of concentration was investigated by varying it from 5 to 10 wt % using the CO_2–DBU-based solvent system and water as the coagulating solvent. Samples with lower concentrations (1, 2, 3, 4 wt %) were unstable during the coagulation step and were therefore not further analyzed. The results obtained showed a linear-like increase of the apparent density from 0.08 to 0.12 g/cm^3 as the cellulose concentration was increased from 5 to 10 wt %. These results are consistent with previous reports using other solvents.(5,21)

Upon replacing water with methanol as the coagulating solvent, while keeping all the other processing parameters constant, a gradual increase of the apparent density was observed from 0.07 to 0.08 g/cm^3 as the cellulose concentration was increased from 5 to 10 wt %. As seen in Figure 1, for the same cellulose concentration, methanol-coagulated aerogels had lower densities compared to their water-coagulated counterparts. As we observed a difference in the apparent density of the aerogels by simply changing the coagulating solvent, other solvents such as ethanol and isopropanol were investigated. In addition, in one approach the coagulation process was carried out in the absence of any added nonsolvent (referred to here as the no-solvent-coagulated aerogel). In this case, the coagulation was allowed to proceed in the DBU–DMSO solvent mixture after the release of CO_2, without any addition of a nonsolvent. After coagulation was complete, the wet sample was then washed repeatedly using methanol to remove the DMSO and DBU followed by a solvent exchange with water to allow for freeze-drying. The comparison of all these solvents on the apparent densities

using 5 wt % MCC is shown in Figure S1. Considering their standard deviation, the obtained results are similar with apparent density values between 0.07 and 0.08 g/cm^3. Methanol was selected for further experiments investigating bases other than DBU in the solvent system, because it showed the least tendency to disrupt the solubilized cellulose surface during the coagulation step, as well as its ease of recovery. Furthermore, alcohols show an acceptable solvent type according to the GSK solvent sustainability guide.(40) For an investigation of the effect of the superbase on the apparent density, cellulose was solubilized (MCC, 5 wt %) using other superbases (TMG and DBN) as described in the Experimental Section using methanol for coagulation. From the results obtained (see Figure S2), similar apparent density values ranging between 0.05 and 0.07 g/cm^3 were obtained.

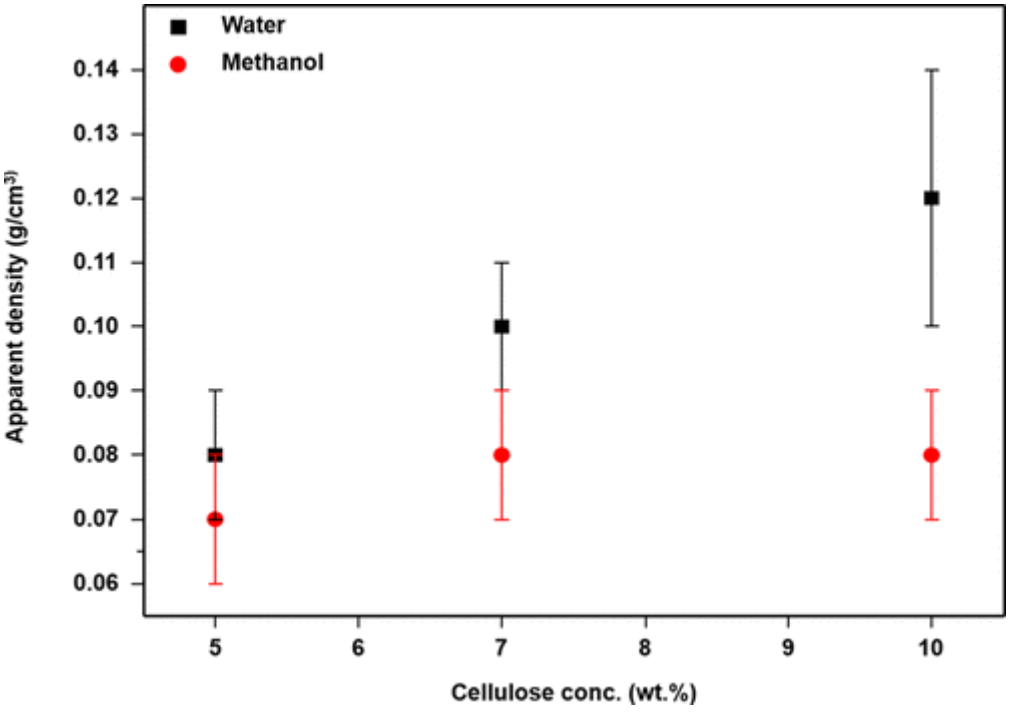

Figure 1. Effect of cellulose concentration on the apparent density of the obtained aerogel.

The porosity of the aerogels was calculated using a common approach,(21,41,42) as follows:

$$\text{porosity}\ (\%) = 100 \times \left(1 - \frac{\rho_{\text{apparent}}}{\rho_{\text{skeletal}}}\right)$$

In the equation, $\rho_{apparent}$ is the calculated apparent density of the aerogel, and $\rho_{skeletal}$ is the true density of microcrystalline cellulose, which is approximately 1.5 g/cm^3.(22)

The obtained porosity results (see Table1), which are in agreement with those of density, gave higher porosity for lower-density samples. The effect of changing the coagulating solvent on the porosity is as follows: water (94%) < methanol, ethanol, isopropanol, no solvent (95%). The highest porosity of 97% was obtained for TMG-based aerogels followed by DBN (96%).

Table 1. Summary of the Processing Conditions and Properties of Cellulose Aerogels from the CO_2 Switchable Solvent System

sample	coagulating solvent	apparent density (g/cm^3)	porosity (%)	pore size (μm)	BET specific surface area (m^2/g)
MCC-5%, DBU	**water**	**0.08 ± 0.01**	**95**	**1.1 ± 0.3**	
MCC-7%, DBU	**water**	**0.10 ± 0.01**	**94**	**2.2 ± 0.4**	
MCC-10%, DBU	**water**	**0.12 ± 0.02**	**92**	**1.6 ± 0.3**	
MCC-5%, DBU	**methanol**	**0.07 ± 0.01**	**95**	**1.2 ± 0.2**	**24 ± 1**
MCC-7%, DBU	**methanol**	**0.08 ± 0.01**	**95**	**1.6 ± 0.2**	**19 ± 1**
MCC-10%, DBU	**methanol**	**0.08 ± 0.01**	**95**	**1.4 ± 0.2**	**26 ± 1**
MCC-5%, DBU	**ethanol**	**0.08 ± 0.01**	**95**	**1.5 ± 0.2**	
MCC-5%, DBU	**isopropanol**	**0.08 ± 0.01**	**95**	**1.2 ± 0.1**	
MCC-5%, DBU	**no-solvent**	**0.08 ± 0.01**	**95**	**1.3 ± 0.3**	
MCC-5%, TMG	**methanol**	**0.05 ± 0.01**	**97**	**3.3 ± 0.5**	
MCC-5%, DBN	**methanol**	**0.06 ± 0.01**	**96**	**4.5 ± 0.7**	
MCC-5%, TMG	**ethanol**	**0.06 ± 0.03**	**96**	**4.2 ± 0.6**	
CP-3%, DBU	**water**	**0.10 ± 0.02**	**93**	**0.6 ± 0.1**	
CP-3%, DBU	**ethanol**	**0.11 ± 0.02**	**93**	**1.1 ± 0.3**	

Morphology and Pore Size

The morphology of the resulting aerogels was studied using scanning electron microscopy (SEM). As with the other basic properties of the aerogels, the effect of the cellulose concentration, coagulating solvents, as well as the superbase on the morphology of the aerogels was investigated. For the DBU-based aerogel and using water as the coagulating solvent, the cellulose concentration was increased from 5 to 10 wt %. The resulting SEM images for 5 wt % are shown in Figure 2; the other concentrations are displayed in the Supporting Information (Figures S3 and S4).

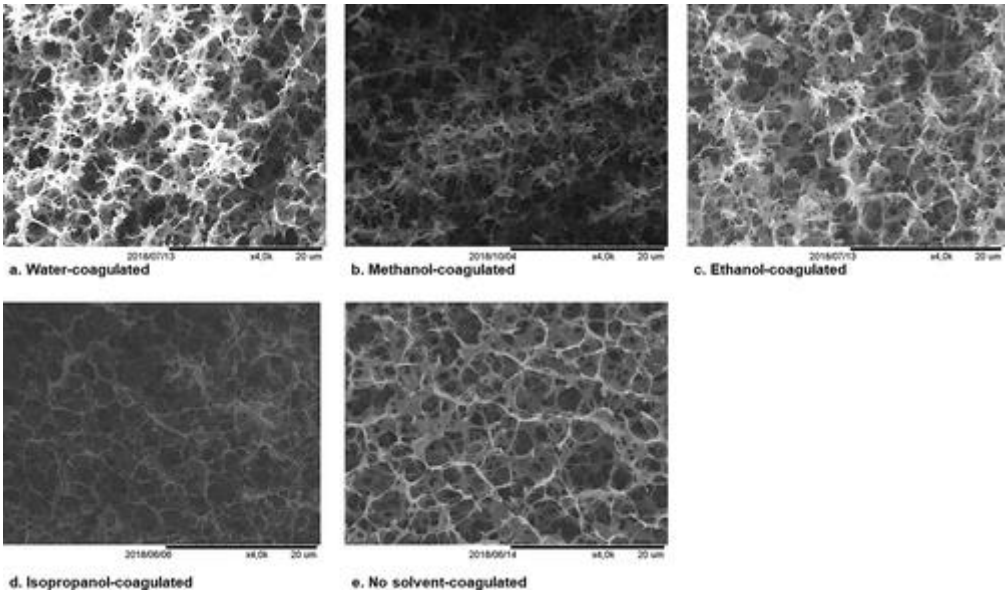

Figure 2. Comparison of SEM images of cellulose (5 wt % MCC) aerogels obtained via freeze-drying (cellulose solubilized in DBU–CO_2 solvent system and coagulated using various solvents).

As can be seen from Figure 2, highly open and interconnected large macroporous cellulose networks with pore walls of around 200–500 nm (estimated from SEM measurements) can be observed, which should be considered as an estimation as the procedure is relatively error prone. These nonporous pore walls probably resulted from ice crystal growth during the freeze-drying step, which causes compactness of the cellulose fibers. This morphology is typical for freeze-dried aerogel samples and similar to those reported by Budtova et al.(21) However, these nonporous walls appeared slightly thinner compared to those in their report. Also, the much finer nanofiber network that is characteristic of supercritical CO_2-dried aerogels(19,20) is not observed, being most likely destroyed during the freeze-drying process because of ice growth during water freezing. A similar morphology was observed when water was replaced with methanol as the coagulating solvent (see Figure 2b). The SEM images for investigations at 7 and 10 wt % are included in the Supporting Information (Figures S5 and S6). Furthermore, using 5 wt % cellulose (MCC), the effect of other coagulating solvents such as ethanol, isopropanol, as well as no solvent on the morphology of the aerogels was investigated. For better comparison, the SEM images of ethanol- and isopropanol-coagulated aerogels are displayed in Figure 2c,d, respectively. These results show similar morphologies as previously described for water- and methanol-coagulated samples. A more uniform and homogeneous morphology was obtained when coagulation of the sample was done without any addition of a nonsolvent (see Figure 2e).

In addition, the effect of the superbase on the aerogel morphology was investigated. Using 5 wt % cellulose and methanol as coagulating solvent, the SEM images for the aerogels using TMG and DBN are shown in Figures S7 and S8. The results show a difference in the morphology compared to the DBU–solvent-based aerogel (see also Figure 2b and compare Figure 3). In the DBN–solvent-based aerogel, the interconnected macroporous cellulose networks are arranged in a “ridgelike” manner with about 8.2 ± 0.8 μm separation between the

“ridges”. Between these ridges, a similar morphology as described for the DBU–solvent samples can be observed. In the TMG–solvent samples, a mixture of ridgelike-arranged large pores and the typical observed open and random large macroporous cellulose network is observed. When methanol was replaced with ethanol and using TMG as superbase (see Figure 3), the ridgelike morphology similar to that of DBN–methanol aerogel could be seen more clearly.

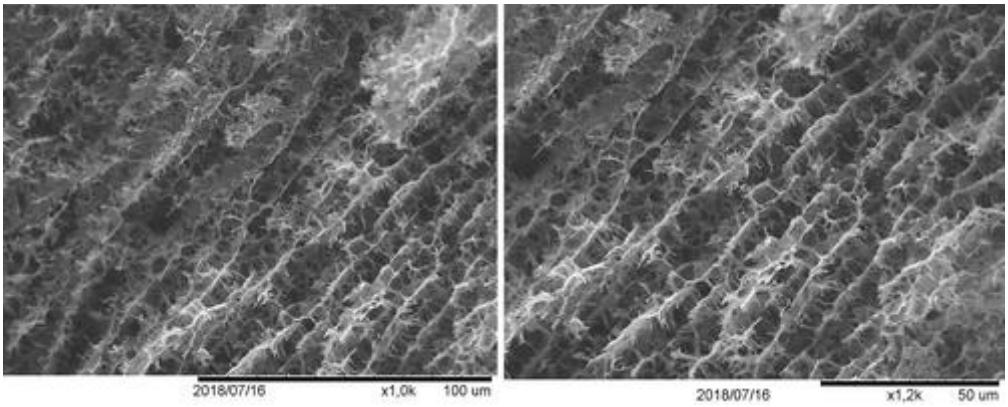

Figure 3. SEM images of cellulose (5 wt % MCC) aerogels obtained via freeze-drying (cellulose solubilized in a TMG–CO_2 solvent system and coagulated using ethanol).

While it will require more detailed studies to fully describe these observed changes, it can be concluded that the solvents as well as their composition can have an influence on the morphologies of the aerogels. This slight variation can therefore be applied for tuning the morphology for a given application. Investigation on cellulose pulp (CP) using water or ethanol for coagulation and DBU as a superbase gave similar morphologies (see Figures S9 and S10) compared to MCC. However, the CP aerogels showed an improved resistance to breakage when compressed by hand compared to MCC aerogels, probably due to a higher molecular weight of the cellulose pulp.

The pore size was estimated from the SEM data as described in the Experimental Section, keeping in mind that this results in a relatively high error margin and can only be used to estimate the range of the pore size, especially for large macropores as observed in the present study. A total of 60 pores was considered for each sample. More accurate methods, such as nitrogen adsorption (Barrett–Joyner–Halenda, BJH approach), do not allow the estimation of a wide range of pore size, while mercury porosimetry faces the limitation of compressing the aerogel pores and not being able to enter the pores.(21) Therefore, SEM was used as a fast approach for estimating the pore size range. The effect of the various processing parameters such as cellulose concentration, coagulating solvents, and superbase on the pore size was investigated. Using water as a coagulating solvent and DBU as a superbase in the solvent system, the cellulose concentration was varied (5, 7, and 10 wt %). The obtained results (Figure 4) show that the pore size ranged between 1.2 and 2.2 µm and does not show a clear trend with varying cellulose concentrations.

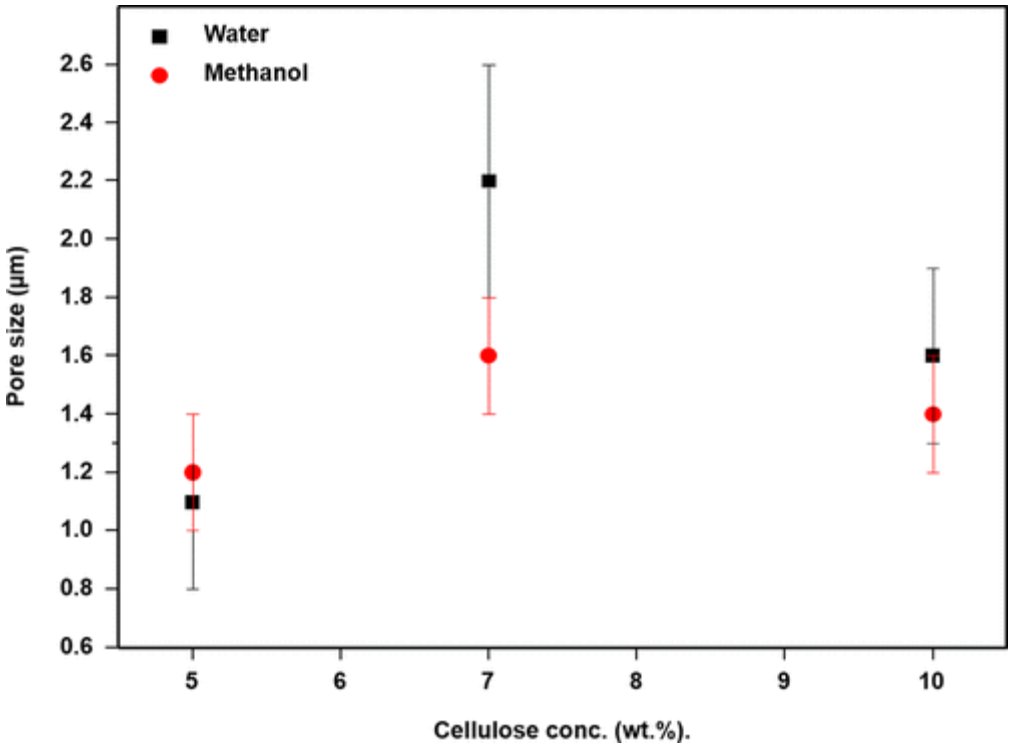

Figure 4. Effect of cellulose concentration on the pore size of cellulose aerogels using DBU as a superbase.

However, it is important to point out that, from our observation, coagulation with water led to a less controlled coagulation process. In contrast to water, the lower density of methanol compared to DMSO–DBU led to a more stable process. Therefore, another attempt was made using methanol as the coagulating solvent, and the results are included in Figure 4. As can be seen, the pore size remained fairly constant (1.2–1.6 µm) as the cellulose concentration was increased from 5 to 10 wt %. These results are somewhat different to those reported by Budtova et al.,(21) where a decrease in pore size was observed with increasing cellulose concentration. As described in their report, an increasing cellulose concentration led to a decrease in the pore size, while the pore walls remained fairly constant. However, we observed that an increased cellulose concentration also led to an increase in the thickness of the pore walls from about 200 to 500 nm as estimated from SEM measurements. Such differences are not unusual, considering that the solvents employed play an important role in the aerogel morphology as shown in the works of Liebner et al.(23) As described by these authors, ionic liquids, which were employed by Budtova et al.,(21) follow a one-step phase separation mechanism for the cellulose network formation, whereas we proposed that the CO_2 switchable solvent rather follows a two-step phase separation mechanism (see our Proposed Mechanism of Cellulose Network Formation section).

For a better picture of the effect of the coagulating solvent on the pore size and using 5 wt % MCC with DBU as superbase, other coagulating solvents such as ethanol, isopropanol, as well as sample without solvent were investigated. The results for these various coagulating solvents on the pore size are shown in Figure S11. The pore size increased in the order 1.1 µm (water) < 1.2 µm (methanol, isopropanol) < 1.3 µm (no solvent) < 1.5 µm (ethanol). Upon consideration of the standard deviation of these values (see Table1), there appears to be little difference in the pore size when the coagulating solvents were changed. However, a size difference of about 0.4 µm can be observed between water and ethanol as the coagulating solvent. Apart from their difference in polarity and structure, the higher density of water (1.0 g/cm^3) compared to ethanol (0.79 g/cm^3) might be responsible for this observation. The higher density of water implies a faster coagulation, as the solvent exchange between water and DMSO–DBU is faster, leading to smaller pore sizes. The role of the solvent density on the pore size was further investigated by using cellulose pulp instead of microcrystalline cellulose. Using water and ethanol as coagulating solvents, the results obtained showed a lower pore size (0.6 µm) for water-coagulated

aerogels compared to 1.1 µm for ethanol-coagulated aerogels (see Figure S12). These results, which are consistent with our previous observations, further support the role of the solvent density on the pore size of the aerogels.

In addition, the effect of the superbase on the pore size was investigated. In this regard, using 5 wt % MCC, the superbases DBU, TMG, and DBN were used for solubilizing cellulose (see the Experimental Section). Coagulation was achieved using methanol, as it is easier to recycle compared to water and also showed the least tendency to disrupt the solubilized cellulose surface during the coagulation step. The results (presented in Figure S13) show an obvious increase in pore size from 1.2 µm when DBU was used, to 3.5 µm in the case of TMG and 4.5 µm for DBN. The reason for this difference is not very clear, and will require further investigation. However, considering the increasing interest for designing tailored cellulose-based materials (aerogel in this case), these results are promising as they give an idea of how to tune the pore size by simply changing the superbase in the solvent system.

In addition, the specific surface area of some aerogels was determined by N_2 adsorption and applying the Brunauer–Emmett–Teller (BET) equation. The BET specific surface area results are included in Table1 (for samples obtained at various cellulose concentrations when DBU- and methanol-coagulation was applied). Data obtained showed specific surface areas between 19 and 26 m^2/g, which are within the range of previous reports for freeze-dried obtained aerogels.(21)

Furthermore, the crystallinity of the aerogels was determined via X-ray diffraction measurements. Samples made with various coagulating solvents as well as different superbases were compared, as shown in Figure 5.

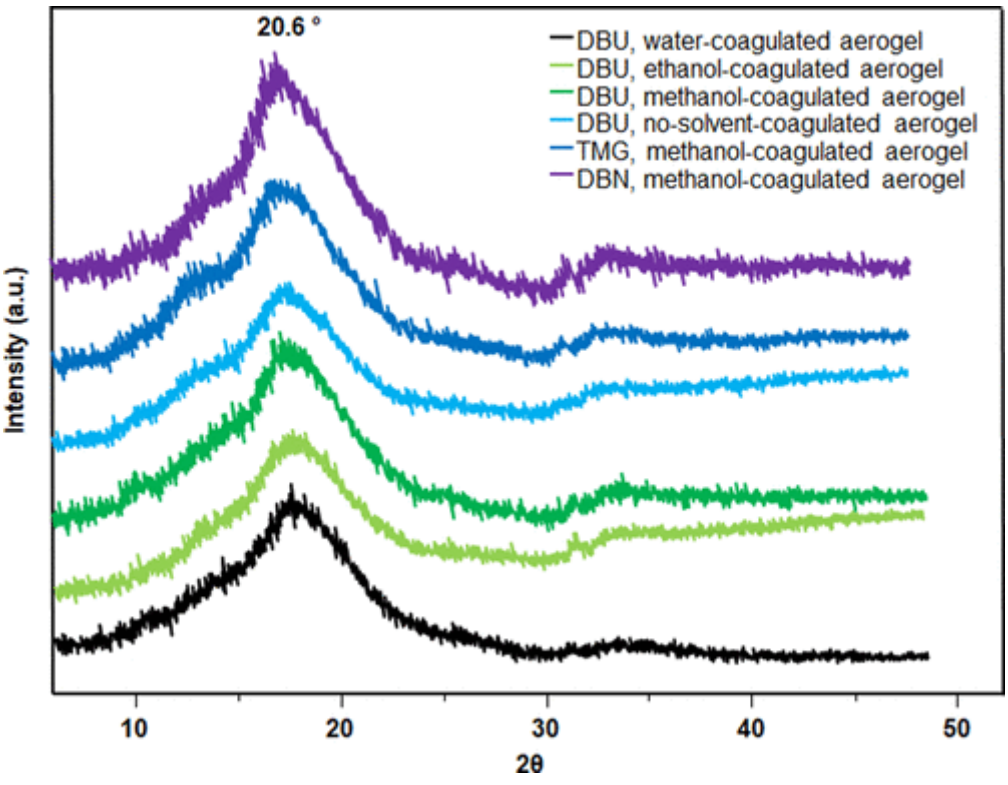

Figure 5. XRD data of cellulose (5 wt % MCC) aerogels obtained via freeze-drying under various processing conditions.

The obtained results showed broad diffraction 2θ peaks at 20.6°, characteristic of a more amorphous cellulose.(38,43) Furthermore, the aerogel coagulated with methanol and using DBU as superbase was compared with the native cellulose (MCC) using infrared spectroscopy (see Figure S14). The obtained results showed that no newly introduced peaks and also no characteristic peaks from the solvent system are visible (DBU and DMSO),

thus showing that no chemical modification occurred during the preparation process. However, an obvious shift and decrease of the O–H stretching vibration peak from 3301 cm^{-1} in the native MCC to 3395 cm^{-1} in the aerogel was noticed. This can be attributed to the decreased *hydrogen* bonding in the aerogel sample compared to the native cellulose. Other observed differences between the spectra are associated with their difference in crystalline structure. Thus, the disappearance of the "crystalline band" peak at 1432 cm^{-1} found in the native cellulose is replaced by an appearance of the "amorphous band" at 898 cm^{-1} in the aerogel sample.(43)

Finally, the recovery of the solvent system was demonstrated (see the Experimental Section for details). Through cyclohexane extraction from the DMSO–DBU–$DBUH^+/HCO_3^-$ mixture, 60% of pure DBU could be recovered. The very low solubility of DBU in cyclohexane means an intensive extraction was required (up to 6 separate extractions to reach 60% recovery); thus, an automated extraction would greatly improve this step. On the other hand, 90% of the DMSO could be recovered via vacuum distillation (25 mbar, 90 °C). A comparison of the pure and recovered solvent was done using infrared spectroscopy (see Figures S15 and S16) and showed no structural differences. In addition, the recovered solvent system (DMSO and DBU) was used for another solubilization of cellulose (5 wt %) and showed no obvious difference. The demonstration of recovery and reuse of the solvent is a very important consideration for sustainability and makes the process appealing for future sustainable cellulose aerogel preparation.

Conclusions

We have reported an easy and sustainable approach for the preparation of cellulose aerogels from the DBU–CO_2 switchable solvent system. Cellulose was first solubilized within 15 min at 30 °C, and the aerogels were prepared via the solubilization–coagulation approach followed by freeze-drying to prevent a collapse of the porous structure. Parameters such as cellulose concentration (5, 7, and 10 wt %), coagulating solvents (water, methanol, ethanol, isopropanol, and no-solvent), as well as the superbase (DBU, TMG, and DBN) on the properties of the aerogels (density, porosity, pore size, and morphology) were investigated. Results obtained showed that increasing cellulose concentrations from 5 to 10 wt % generally led to an increase in the density and an associated decrease in porosity. Upon variation of the various processing parameters, porosity values obtained ranged between 92% and 97%, with densities between 0.05 and 0.12 g/cm^3. Furthermore, from scanning electron microscopy (SEM), all investigated coagulated solvents showed a random open large macroporous cellulose network morphology with thin cell walls ranging between 200 and 500 nm and pore size between 1.2 and 2.2 µm. However, the aerogels coagulated without solvent showed a more homogeneous large macroporous cellulose network. Furthermore, changing the superbase resulted in a difference in the morphology as well as the pore size of the aerogels. A ridgelike-arranged large macroporous cellulose network was observed for DBN and TMG that was absent in the case of DBU. In addition, the pore size could be tuned from 1.2 µm (DBU) to 3.3 µm (TMG) or 4.5 µm for DBN. The calculated BET specific surface areas ranged between 19 and 26 m^2/g as cellulose concentration was varied between 5 and 10 wt % for methanol-coagulated aerogel samples.

Furthermore, the recovery (DBU 60%, DMSO 90%) and reuse of the solvent system was demonstrated. Finally, the reported detailed study of the effect of the various processing conditions on the properties of the obtained aerogels will allow for a design of cellulose aerogels to suit a given application.

Acknowledgments

K.N.O. would like to thank the EU for Ph.D. funding under the Horizon 2020 Marie Sklodowska-Curie ITN Project EJD-FunMat (Project 641640). H.C. and M.A.R.M. are also thankful for this funding.

References

1. Klemm, D.; Heublein, B.; Fink, H.-P.; Bohn, A. Cellulose: fascinating biopolymer and sustainable raw material. *Angew. Chem., Int. Ed.* **2005**, *44*, 3358– 3393, DOI: 10.1002/anie.200460587
2. Sescousse, R.; Gavillon, R.; Budtova, T. Wet and dry highly porous cellulose beads from cellulose–NaOH–water solutions: influence of the preparation conditions on beads shape and encapsulation of inorganic particles. *J. Mater. Sci.* **2011**, *46*, 759– 765, DOI: 10.1007/s10853-010-4809-5

3. Trygg, J.; Fardim, P.; Gericke, M.; Mäkilä, E.; Salonen, J. Physicochemical design of the morphology and ultrastructure of cellulose beads. *Carbohydr. Polym.* **2013**, *93*, 291– 299, DOI: 10.1016/j.carbpol.2012.03.085
4. Druel, L.; Niemeyer, P.; Milow, B.; Budtova, T. Rheology of cellulose-[DBNH][CO_2Et] solutions and shaping into aerogel beads. *Green Chem.* **2018**, *20*, 3993– 4002, DOI: 10.1039/C8GC01189C
5. Innerlohinger, J.; Weber, H. K.; Kraft, G. Aerocellulose: Aerogels and Aerogel-like Materials made from Cellulose. *Macromol. Symp.* **2006**, *244*, 126– 135, DOI: 10.1002/masy.200651212
6. Liebner, F.; Rosenau, T. *Functional Materials from Renewable Sources*; American Chemical Society: Washington, DC, **2012**.
7. Pekala, R. W. Organic aerogels from the polycondensation of resorcinol with formaldehyde. *J. Mater. Sci.* **1989**, *24*, 3221– 3227, DOI: 10.1007/BF01139044
8. Bock, V.; Emmerling, A.; Saliger, R.; Fricke, J. Structural Investigation of Resorcinol Formaldehyde and Carbon Aerogels Using SAXS and BET. *J. Porous Mater.* **1997**, *4*, 287– 294, DOI: 10.1023/A:1009681407649
9. Thapliyal, P. C.; Singh, K. Aerogels as Promising Thermal Insulating Materials: An Overview. *J. Mater.* **2014**, *2014*, 1– 10, DOI: 10.1155/2014/127049
10. Wu, Z.-Y.; Li, C.; Liang, H.-W.; Chen, J.-F.; Yu, S.-H. Ultralight, flexible, and fire-resistant carbon nanofiber aerogels from bacterial cellulose. *Angew. Chem., Int. Ed.* **2013**, *52*, 2925– 2929, DOI: 10.1002/anie.201209676
11. García-González, C. A.; Alnaief, M.; Smirnova, I. Polysaccharide-based aerogels—Promising biodegradable carriers for drug delivery systems. *Carbohydr. Polym.* **2011**, *86*, 1425– 1438, DOI: 10.1016/j.carbpol.2011.06.066
12. Ulker, Z.; Erkey, C. An emerging platform for drug delivery: aerogel based systems. *J. Controlled Release* **2014**, *177*, 51– 63, DOI: 10.1016/j.jconrel.2013.12.033
13. Kistler, S. S. Coherent Expanded Aerogels and Jellies. *Nature* **1931**, *127*, 741, DOI: 10.1038/127741a0
14. Kistler, S. S. Coherent Expanded-Aerogels. *J. Phys. Chem.* **1931**, *36*, 52– 64, DOI: 10.1021/j150331a003
15. Liebner, F.; Haimer, E.; Wendland, M.; Neouze, M.-A.; Schlufter, K.; Miethe, P.; Heinze, T.; Potthast, A.; Rosenau, T. Aerogels from unaltered bacterial cellulose: application of scCO_2 drying for the preparation of shaped, ultra-lightweight cellulosic aerogels. *Macromol. Biosci.* **2010**, *10*, 349– 352, DOI: 10.1002/mabi.200900371
16. Pääkkö, M.; Vapaavuori, J.; Silvennoinen, R.; Kosonen, H.; Ankerfors, M.; Lindström, T.; Berglund, L. A.; Ikkala, O. Long and entangled native cellulose I nanofibers allow flexible aerogels and hierarchically porous templates for functionalities. *Soft Matter* **2008**, *4*, 2492, DOI: 10.1039/b810371b
17. Zhang, Z.; Sèbe, G.; Rentsch, D.; Zimmermann, T.; Tingaut, P. Ultralightweight and Flexible Silylated Nanocellulose Sponges for the Selective Removal of Oil from Water. *Chem. Mater.* **2014**, *26*, 2659– 2668, DOI: 10.1021/cm5004164
18. Wang, Z.; Liu, S.; Matsumoto, Y.; Kuga, S. Cellulose gel and aerogel from LiCl/DMSO solution. *Cellulose* **2012**, *19*, 393– 399, DOI: 10.1007/s10570-012-9651-2
19. Hoepfner, S.; Ratke, L.; Milow, B. Synthesis and characterisation of nanofibrillar cellulose aerogels. *Cellulose* **2008**, *15*, 121– 129, DOI: 10.1007/s10570-007-9146-8
20. Jin, H.; Nishiyama, Y.; Wada, M.; Kuga, S. Nanofibrillar cellulose aerogels. *Colloids Surf., A* **2004**, *240*, 63– 67, DOI: 10.1016/j.colsurfa.2004.03.007
21. Buchtová, N.; Budtova, T. Cellulose aero-, cryo- and xerogels: towards understanding of morphology control. *Cellulose* **2016**, *23*, 2585– 2595, DOI: 10.1007/s10570-016-0960-8
22. Sun, C. C. True density of microcrystalline cellulose. *J. Pharm. Sci.* **2005**, *94*, 2132– 2134, DOI: 10.1002/jps.20459
23. Pircher, N.; Carbajal, L.; Schimper, C.; Bacher, M.; Rennhofer, H.; Nedelec, J.-M.; Lichtenegger, H. C.; Rosenau, T.; Liebner, F. Impact of selected solvent systems on the pore and solid structure of cellulose aerogels. *Cellulose* **2016**, *23*, 1949– 1966, DOI: 10.1007/s10570-016-0896-z
24. Dorn, S.; Wendler, F.; Meister, F.; Heinze, T. Interactions of Ionic Liquids with Polysaccharides - 7: Thermal Stability of Cellulose in Ionic Liquids and N -Methylmorpholine- N -oxide. *Macromol. Mater. Eng.* **2008**, *293*, 907– 913, DOI: 10.1002/mame.200800153
25. Rosenau, T.; Potthast, A.; Sixta, H.; Kosma, P. *Prog. Polym. Sci.* **2001**, *26*, 1763– 1837, DOI: 10.1016/S0079-6700(01)00023-5
26. Clough, M. T.; Geyer, K.; Hunt, P. A.; Son, S.; Vagt, U.; Welton, T. Ionic liquids: not always innocent solvents for cellulose. *Green Chem.* **2015**, *17*, 231– 243, DOI: 10.1039/C4GC01955E
27. Gericke, M.; Fardim, P.; Heinze, T. Ionic liquids--promising but challenging solvents for homogeneous derivatization of cellulose. *Molecules* **2012**, *17*, 7458– 7502, DOI: 10.3390/molecules17067458
28. Llevot, A.; Dannecker, P.-K.; von Czapiewski, M.; Over, L. C.; Söyler, Z.; Meier, M. A. R. Renewability is not Enough: Recent Advances in the Sustainable Synthesis of Biomass-Derived Monomers and Polymers. *Chem. - Eur. J.* **2016**, *22*, 11510– 11521, DOI: 10.1002/chem.201602068
29. Anastas, P. T.; Warner, J. C. *Green Chemistry: Theory and Practice*; Oxford University Press: Oxford, **1998**.
30. Erythropel, H. C.; Zimmerman, J. B.; Winter, T. M. de; Petitjean, L.; Melnikov, F.; Lam, C. H.; Lounsbury, A. W.; Mellor, K. E.; Janković, N. Z.; Tu, Q.; Pincus, L. N.; Falinski, M. M.; Shi, W.; Coish, P.; Plata, D. L.; Anastas, P. T. The Green ChemisTREE: 20 years after taking root with the 12 principles. *Green Chem.* **2018**, *20*, 1929– 1961, DOI: 10.1039/C8GC00482J
31. Jessop, P. G.; Heldebrant, D. J.; Li, X.; Eckert, C. A.; Liotta, C. L. Green chemistry: Reversible nonpolar-to-polar solvent. *Nature* **2005**, *436*, 1102, DOI: 10.1038/4361102a
32. Zhang, Q.; Oztekin, N. S.; Barrault, J.; Oliveira Vigier, K. de; Jérôme, F. Activation of microcrystalline cellulose in a CO_2-based switchable system. *ChemSusChem* **2013**, *6*, 593– 596, DOI: 10.1002/cssc.201200815
33. Xie, H.; Yu, X.; Yang, Y.; Zhao, Z. K. Capturing CO_2 for cellulose dissolution. *Green Chem.* **2014**, *16*, 2422– 2427, DOI: 10.1039/C3GC42395F
34. Chowdhury, S. A.; Vijayaraghavan, R.; MacFarlane, D. R. Distillable ionic liquid extraction of tannins from plant materials. *Green Chem.* **2010**, *12*, 1023, DOI: 10.1039/b923248f
35. King, A. W. T.; Asikkala, J.; Mutikainen, I.; Järvi, P.; Kilpeläinen, I. Distillable acid-base conjugate ionic liquids for cellulose dissolution and processing. *Angew. Chem., Int. Ed.* **2011**, *50*, 6301– 6305, DOI: 10.1002/anie.201100274
36. Sixta, H.; Michud, A.; Hauru, L.; Asaadi, S.; Ma, Y.; King, A. W. T.; Kilpeläinen, I.; Hummel, M. Ioncell-F: A High-strength regenerated cellulose fibre. *Nord. Pulp Pap. Res. J.* **2005**, *30* (1), 43– 57
37. Onwukamike, K. N.; Tassaing, T.; Grelier, S.; Grau, E.; Cramail, H.; Meier, M. A. R. Detailed Understanding of the DBU/CO_2 Switchable Solvent System for Cellulose Solubilization and Derivatization. *ACS Sustainable Chem. Eng.* **2018**, *6*, 1496– 1503, DOI: 10.1021/acssuschemeng.7b04053
38. Onwukamike, K. N.; Grelier, S.; Grau, E.; Cramail, H.; Meier, M. A. R. Sustainable Transesterification of Cellulose with High Oleic Sunflower Oil in a DBU-CO_2 Switchable Solvent. *ACS Sustainable Chem. Eng.* **2018**, *6*, 8826– 8835, DOI: 10.1021/acssuschemeng.8b01186

39. Söyler, Z.; Onwukamike, K. N.; Grelier, S.; Grau, E.; Cramail, H.; Meier, M. A. R. Sustainable succinylation of cellulose in a CO_2-based switchable solvent and subsequent Passerini 3-CR and Ugi 4-CR modification. *Green Chem.* **2018**, *20*, 214– 224, DOI: 10.1039/C7GC02577G
40. Alder, C. M.; Hayler, J. D.; Henderson, R. K.; Redman, A. M.; Shukla, L.; Shuster, L. E.; Sneddon, H. F. Updating and further expanding GSK's solvent sustainability guide. *Green Chem.* **2016**, *18*, 3879– 3890, DOI: 10.1039/C6GC00611F
41. Shinko, A.; Jana, S. C.; Meador, M. A. Crosslinked polyurea aerogels with controlled porosity. *RSC Adv.* **2015**, *5*, 105329– 105338, DOI: 10.1039/C5RA20788F
42. Du, M.; Mao, N.; Russell, S. J. Control of porous structure in flexible silicone aerogels produced from methyltrimethoxysilane (MTMS): the effect of precursor concentration in sol–gel solutions. *J. Mater. Sci.* **2016**, *51*, 719– 731, DOI: 10.1007/s10853-015-9378-1

43. Ciolacu, D.; Ciolacu, F.; Popa, V. I. Amorphous Cellulose-Structure and Characterization. *Cell. Chem. Technol.* **2011**, *45*, 13– 21

Supporting Information for:

Sustainable approach for Cellulose aerogel preparation from the DBU-CO_2 Switchable Solvent

Kelechukwu N. Onwukamike,[a,b] Laurine Lapuyade,[c] Laurence Maillé,[c] Stéphane Grelier,[b] Etienne Grau,[b] Henri Cramail,[b] Michael A.R. Meier[a*]*

[a] Institute of Organic Chemistry (IOC), Materialwissenschaftliches Zentrum (MZE), Karlsruhe Institute of Technology (KIT), Straße am Forum 7, 76131 Karlsruhe, Germany

[b] Laboratoire de Chimie des Polymères Organiques, Université de Bordeaux, UMR5629, CNRS - Bordeaux INP - ENSCBP, 16 Avenue Pey-Berland, 33607 Pessac Cedex France

[c] Laboratoire des Composites Thermostructuraux (LCTS), Université de Bordeaux-CNRS-Safran-CEA, UMR 5801, 3 Allée de La Boétie, 33600 Pessac, France

Number of pages: 12

Number of figures: 16

I. Effect of coagulating solvent and super base on apparent density of cellulose aerogel

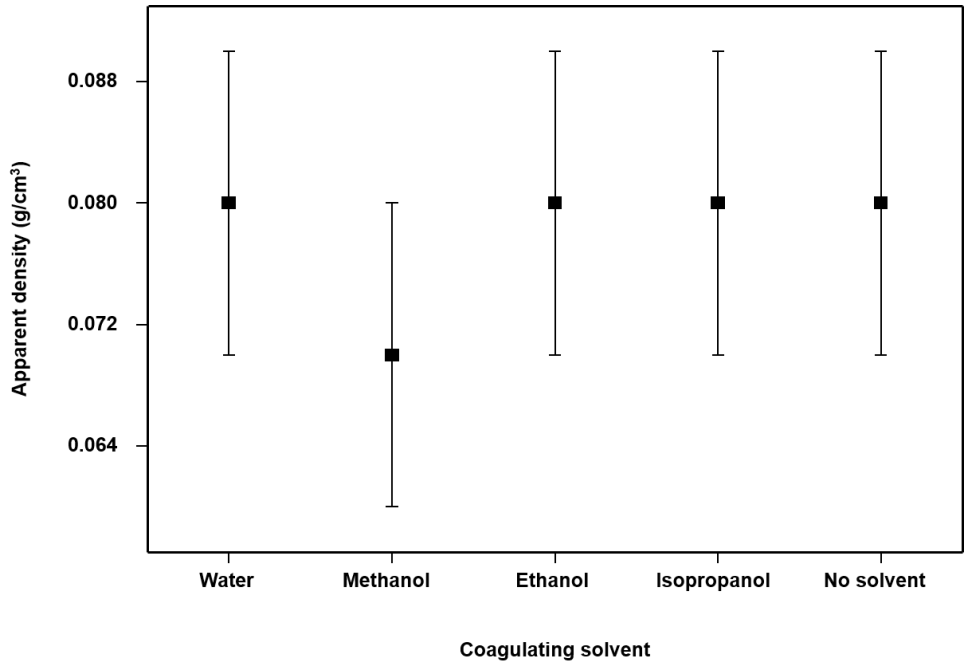

Figure SI 1: Effect of coagulating solvent on the apparent density of cellulose aerogel using 5 wt.% MC and DBU as a super base.

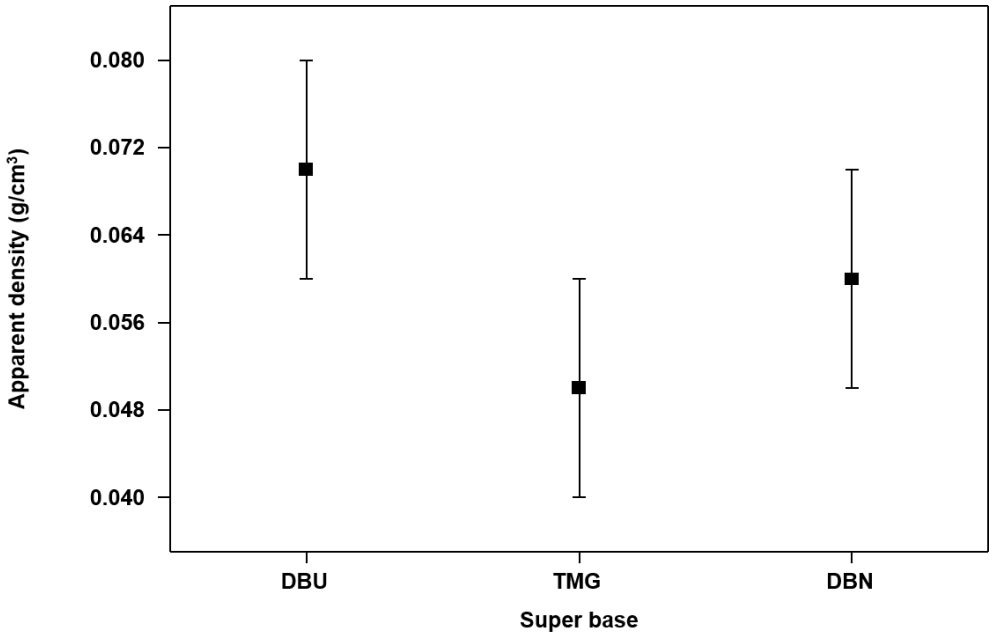

Figure SI 2: Effect of the super base on the apparent density of cellulose aerogel using 5 wt.% MCC and methanol coagulation.

II. Morphology studies *via* SEM of cellulose aerogels under various processing conditions

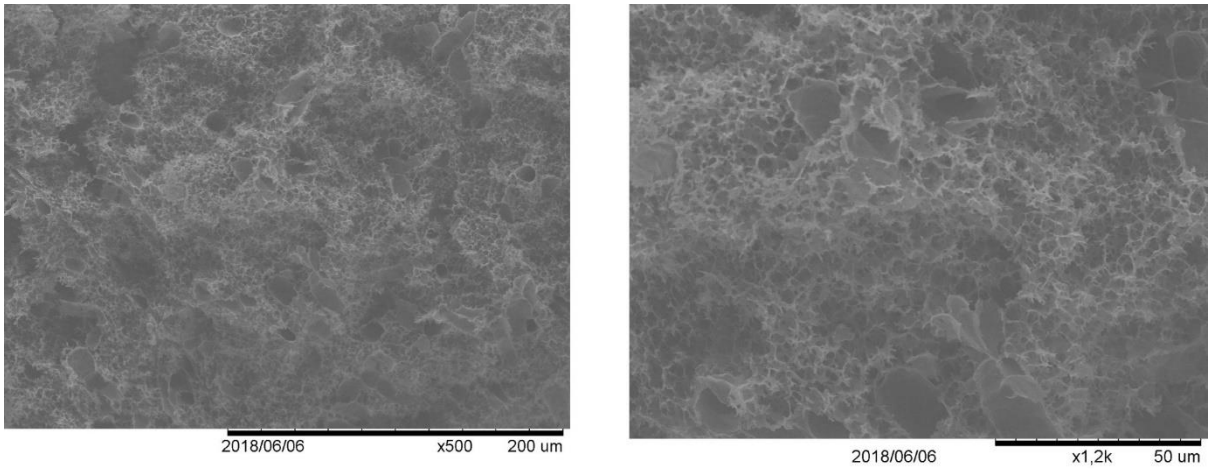

Figure SI 3: SEM image of cellulose aerogel from freeze-drying (using 7 wt.% MCC, DBU as a super base and water coagulation.

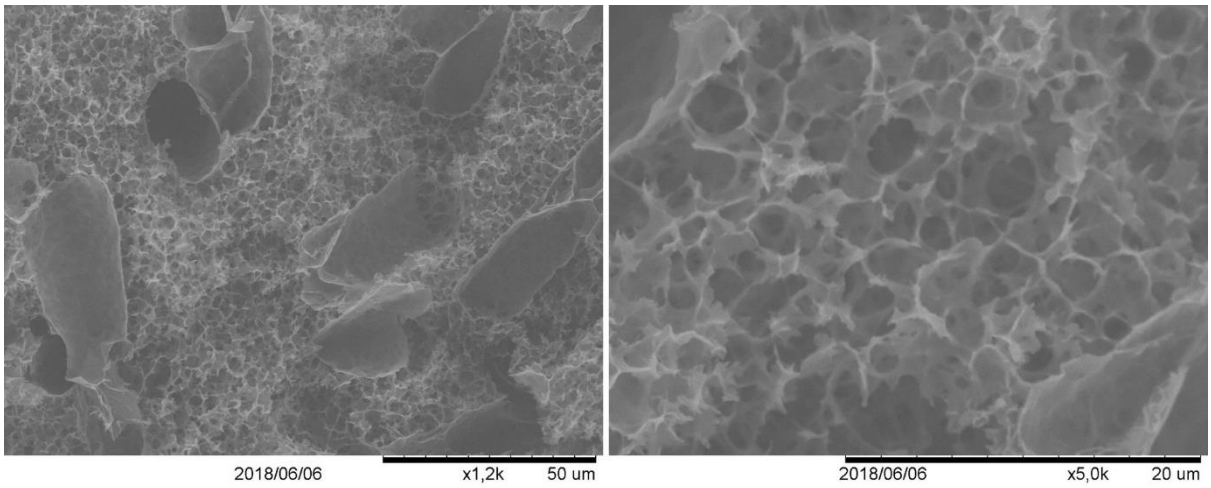

Figure SI 4: SEM image of cellulose aerogel from freeze-drying (using 10 wt.% MCC, DBU as super base and water coagulation.

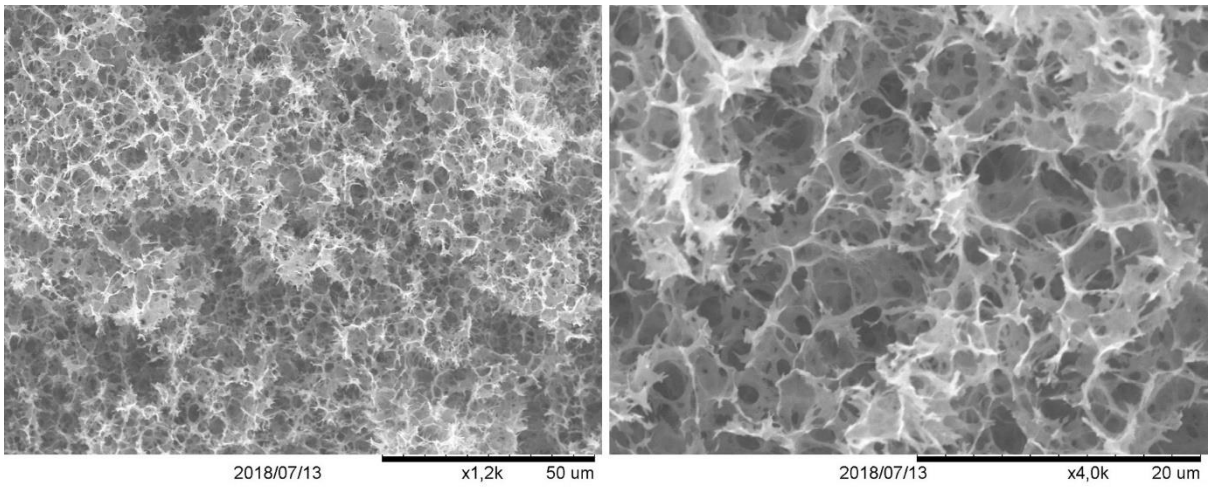

Figure SI 5: SEM image of cellulose aerogel from freeze-drying (using 7 wt.% MCC, DBU as super base and methanol coagulation.

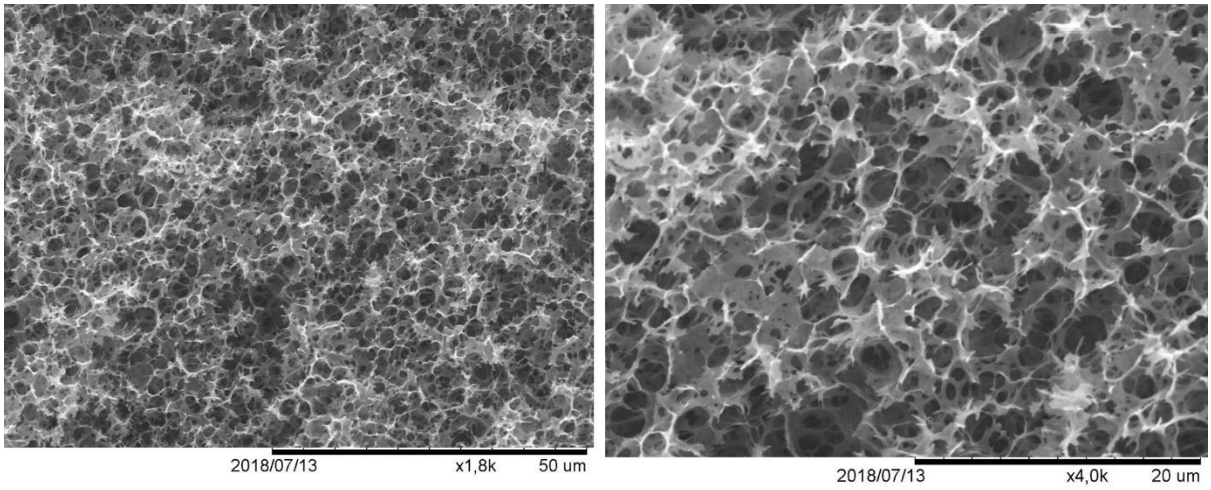

Figure SI 6: SEM image of cellulose aerogel from freeze-drying (using 10 wt.% MCC, DBU as super base and methanol coagulation.

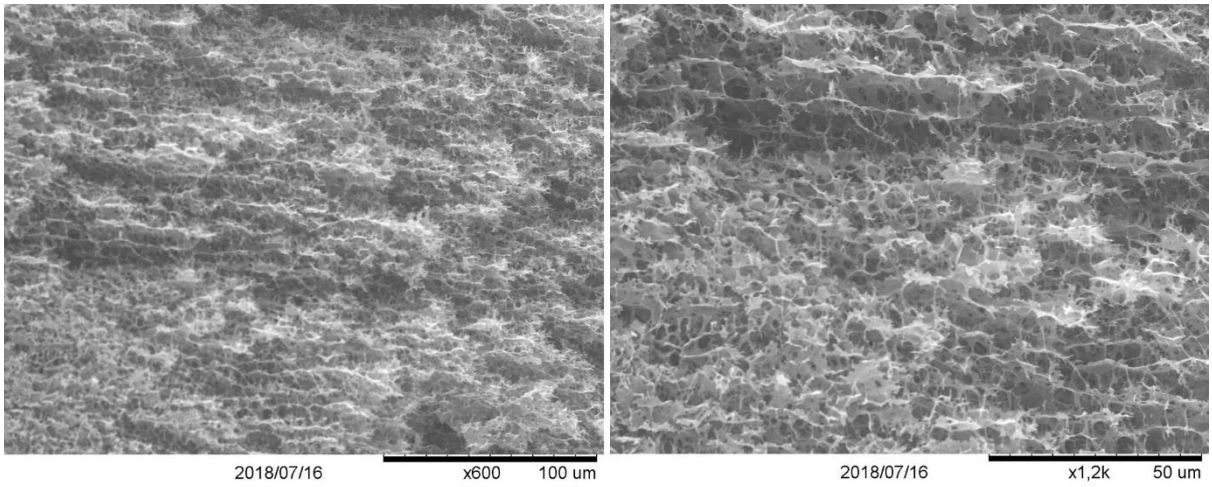

Figure SI 7: SEM image of cellulose aerogel from freeze-drying (using 5 wt.% MCC, TMG as super base and methanol coagulation.

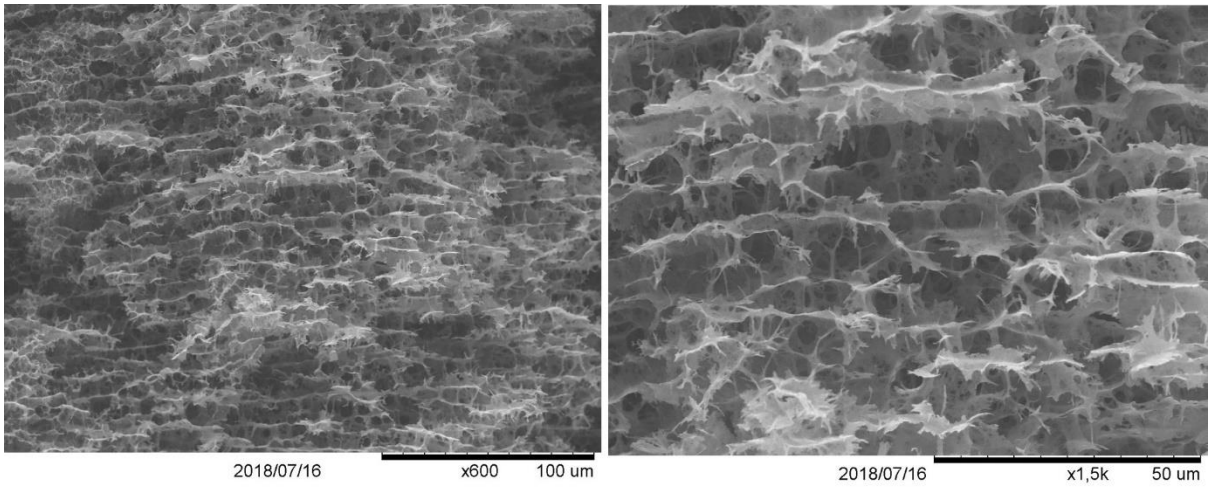

Figure SI 8: SEM image of cellulose aerogel from freeze-drying (using 5 wt.% MCC, DBN as super base and methanol coagulation.

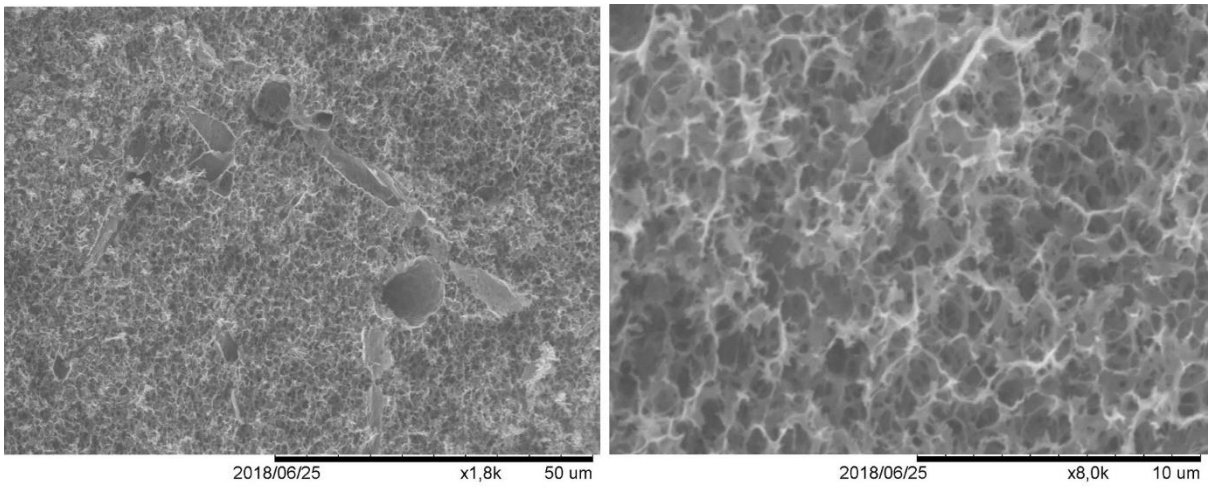

Figure SI 9: SEM image of cellulose aerogel from freeze-drying (using 3 wt.% CP, DBU as super base and water coagulation.

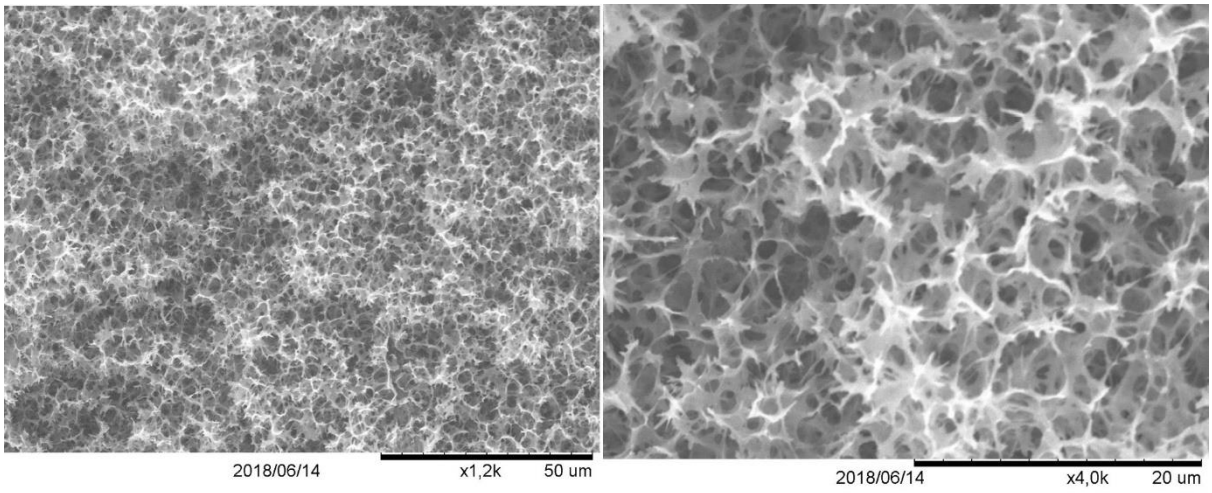

Figure SI 10: SEM image of cellulose aerogel from freeze-drying (using 3 wt.% CP, DBU as super base and ethanol coagulation.

III. Effect of coagulating solvent and super base on pore size of cellulose aerogel

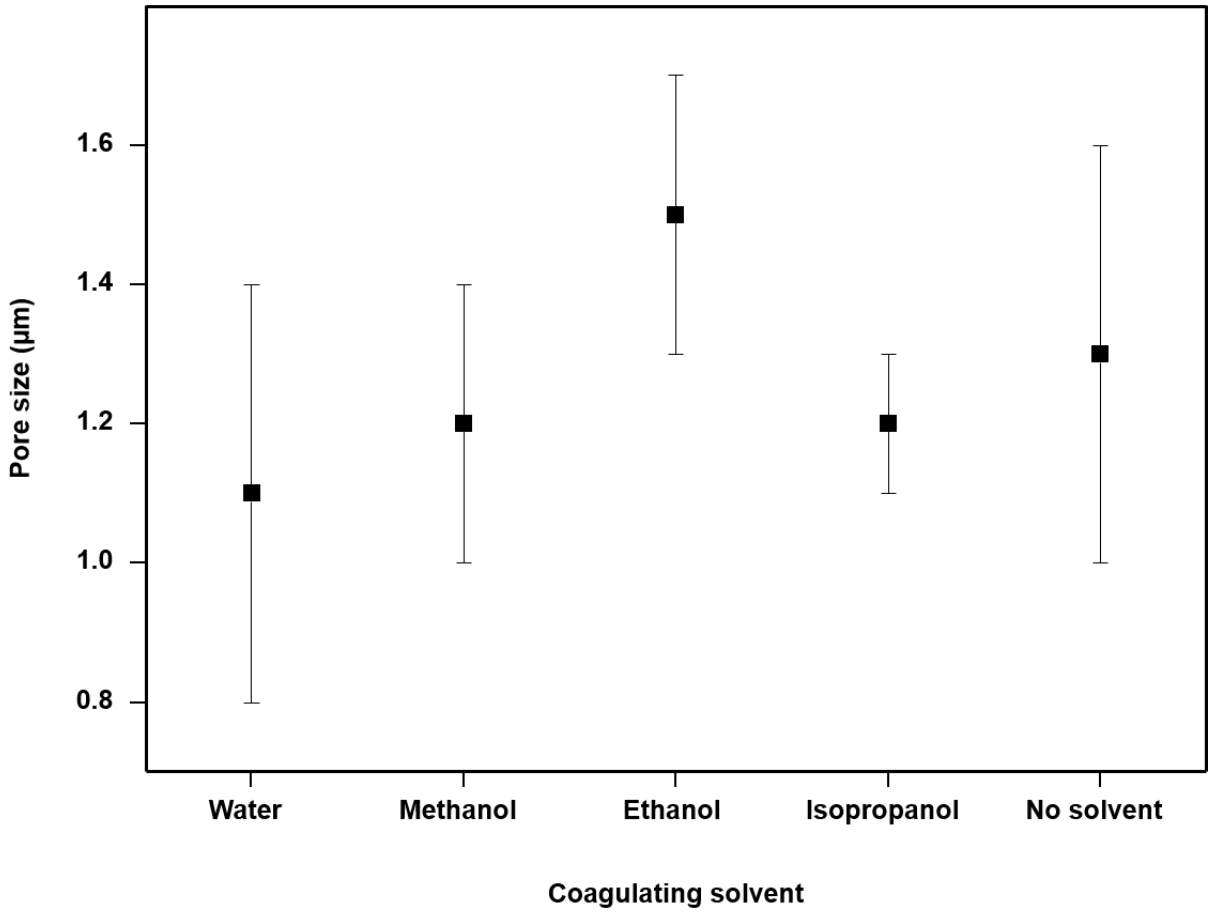

Figure SI 11: Effect of coagulating solvent on the pore size of cellulose aerogel using 5 wt.% MC and DBU as a super base.

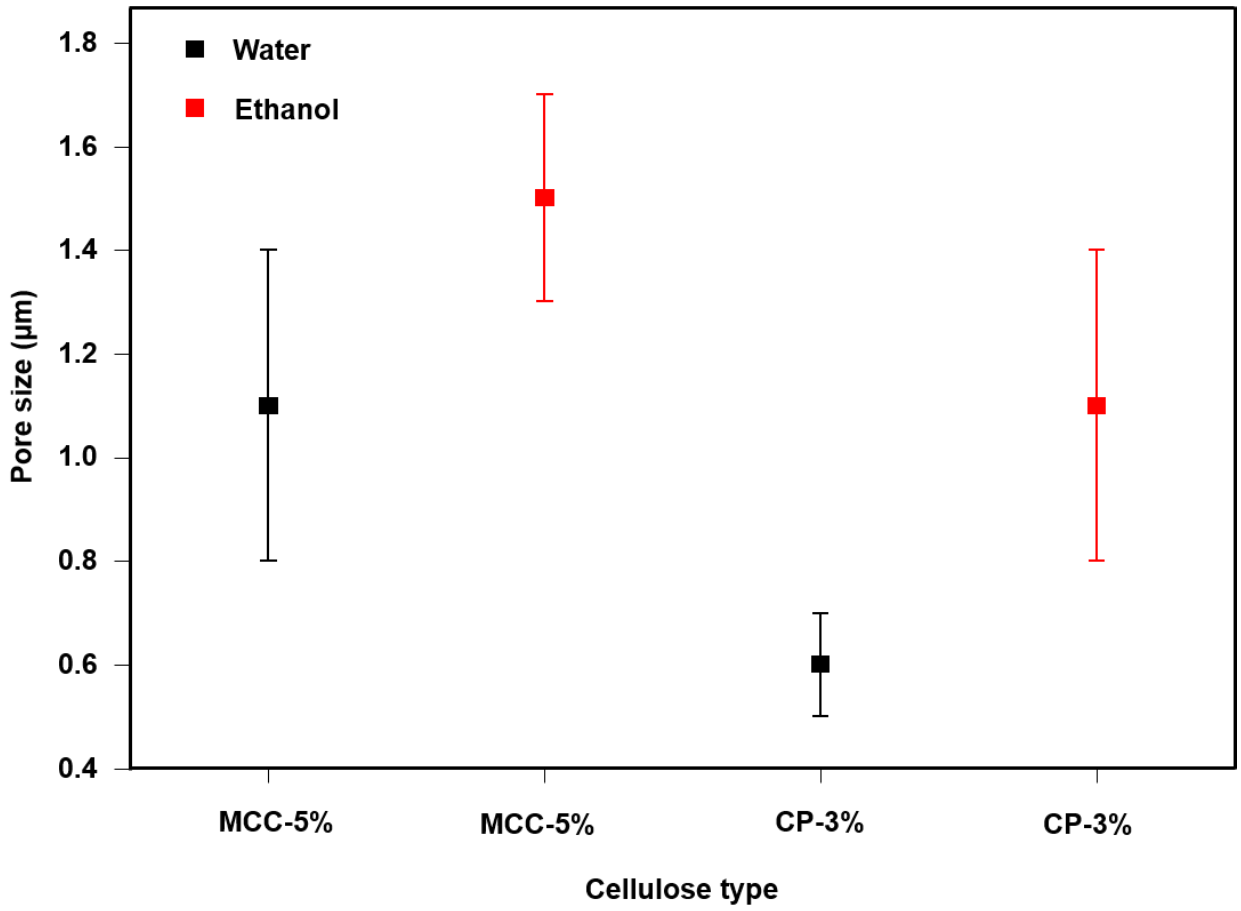

Figure SI 12: Effect of cellulose type and coagulating solvent on the pore size of cellulose aerogel using DBU as a super base.

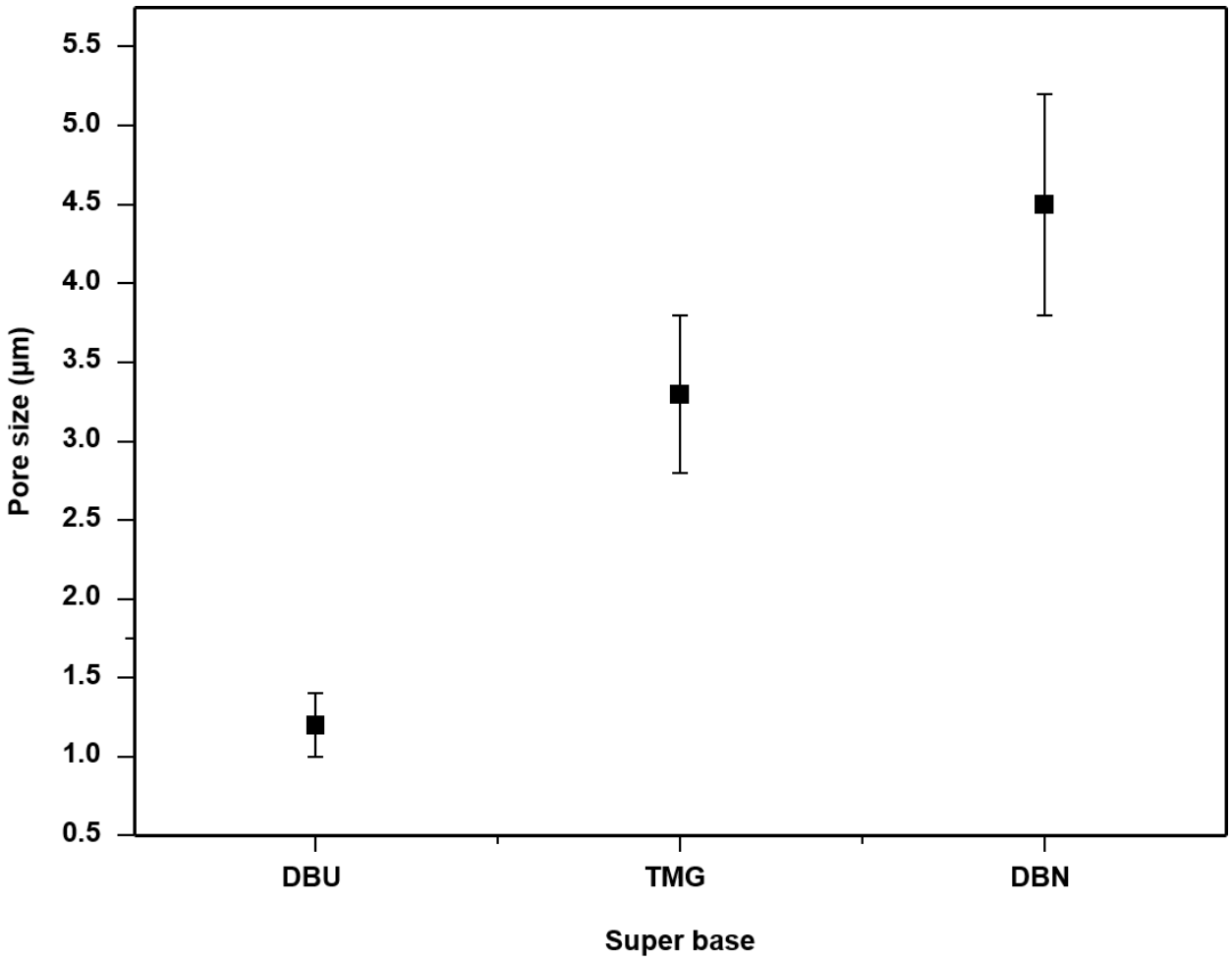

Figure SI 13: Effect of the super base on the porosity of cellulose aerogel using 5 wt.% MCC and methanol coagulation.

IV. FT-IR spectra comparison between native MCC and cellulose aerogel

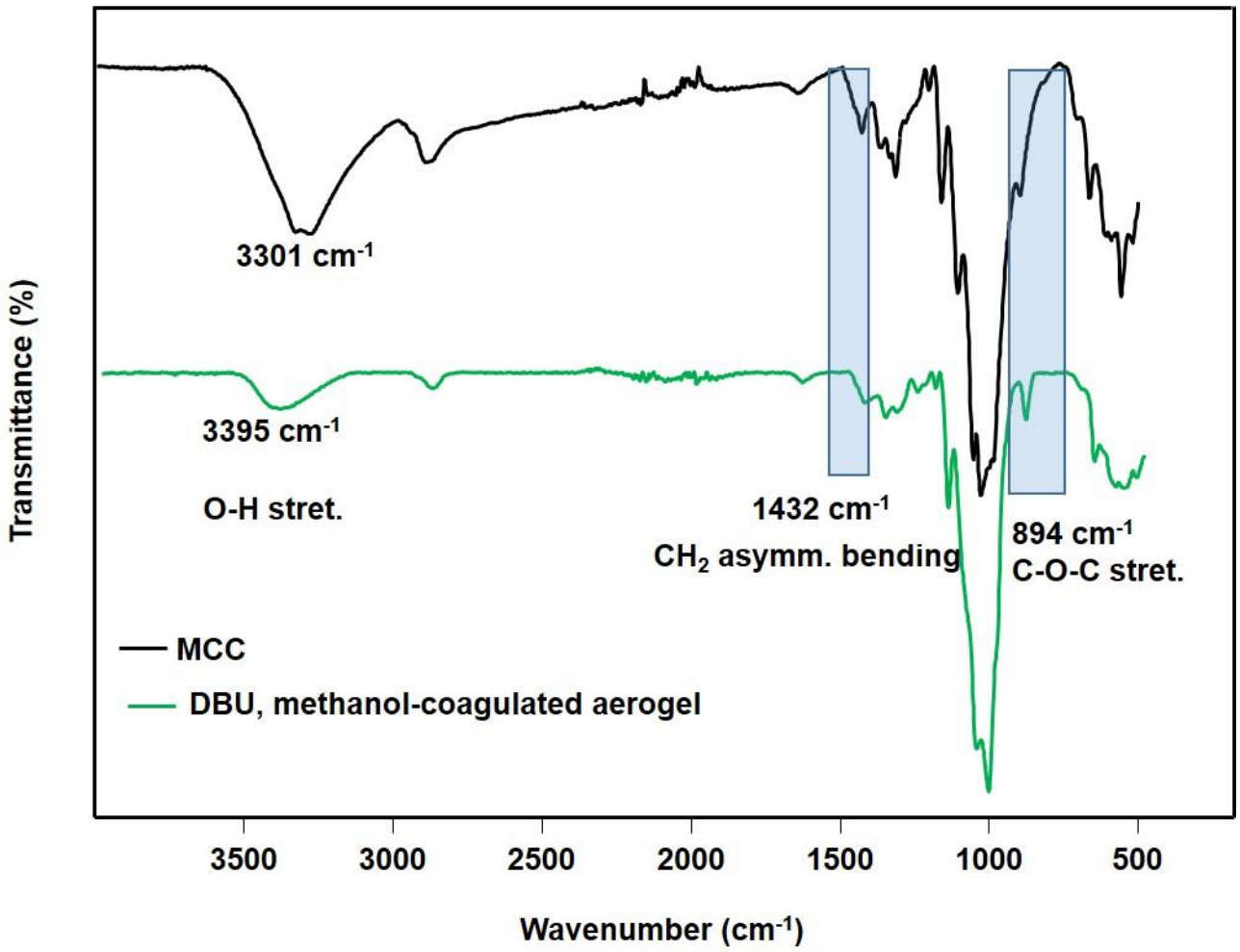

Figure SI 14: FT-IR spectra comparison between MCC and cellulose aerogel from freeze-drying (using 5 wt.% MCC, DBU as super base and methanol coagulation.

V. FT-IR spectra comparison between pure and recovered DBU and DMSO

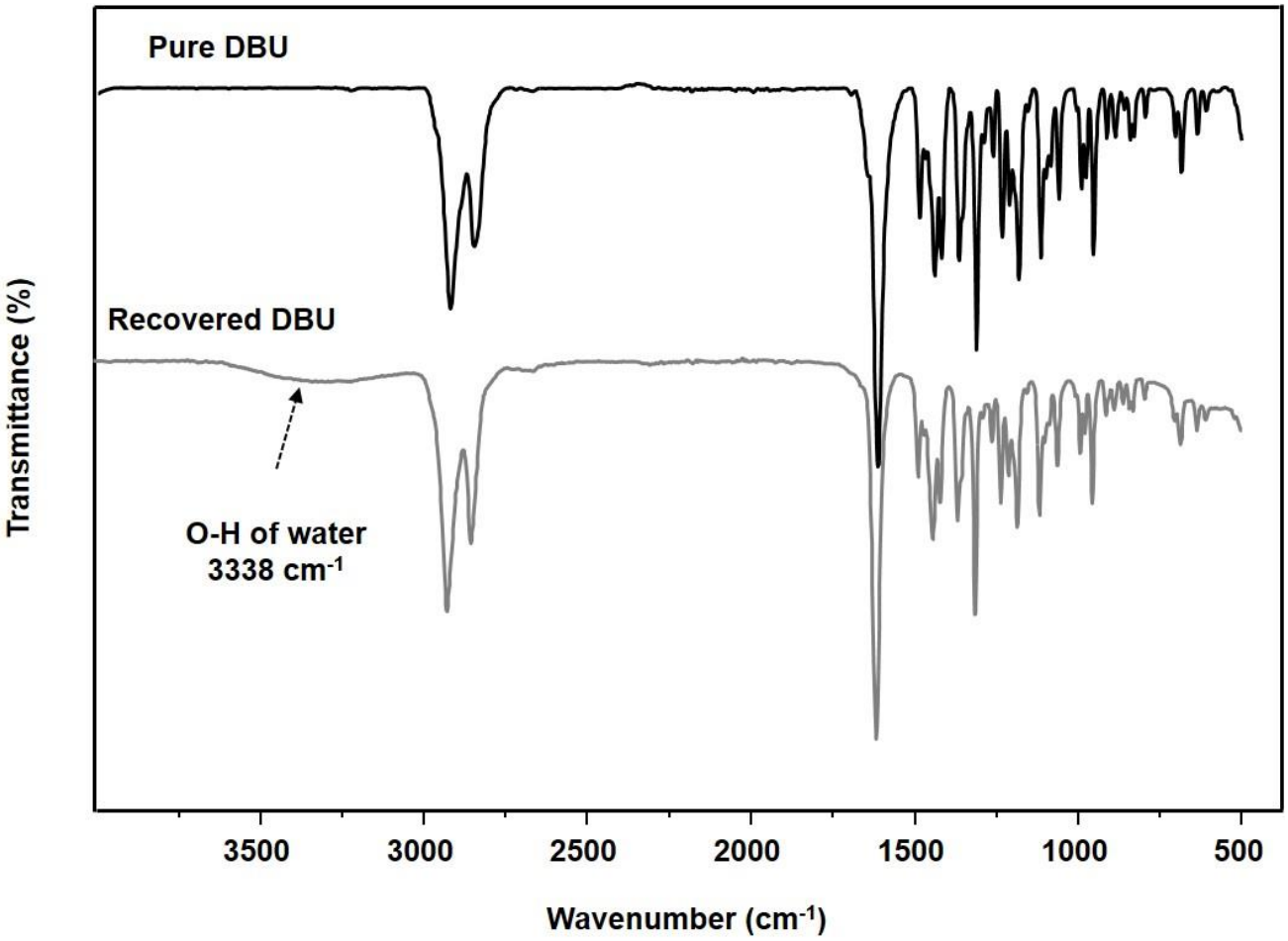

Figure SI 15: FT-IR spectra comparison between pure and recovered DBU (using 5 wt.% MCC, DBU as super base and methanol coagulation).

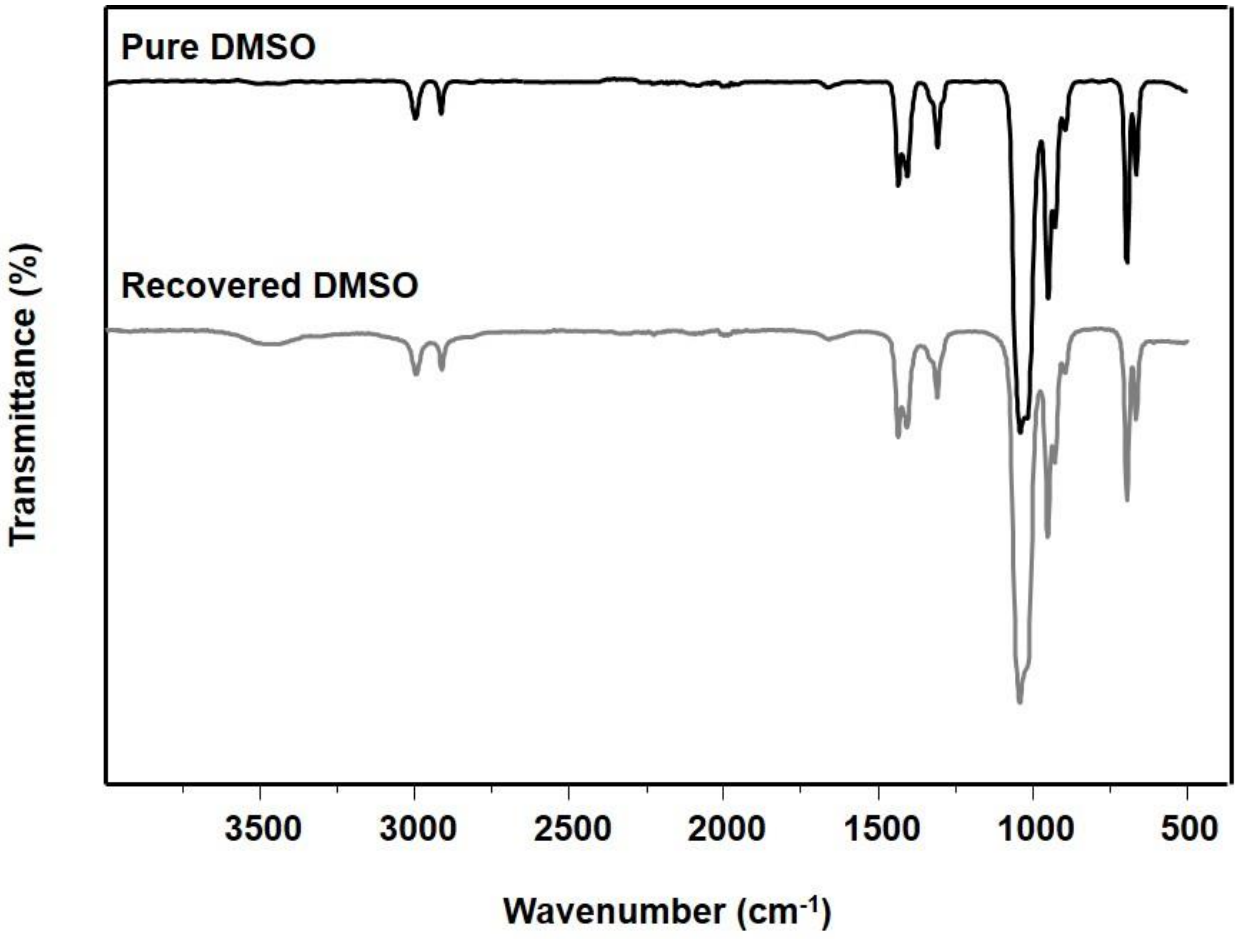

Figure SI 16: FT-IR spectra comparison between pure and recovered DMSO (using 5 wt.% MCC, DBU as super base and methanol coagulation).